https://doi.org/10.5194/egusphere-2025-4898
Preprint. Discussion started: 29 October 2025

A multi-model approach to constrain the atmospheric hydrogen budget

Srinath Krishnan[1], Ragnhild Bieltvedt Skeie[1], Øivind Hodnebrog[1], Gunnar Myhre[1], Maria Sand[1], Marit Sandstad[1], Hannah Bryant[2], Didier A. Hauglustaine[3], Fabien Paulot[4], Michael Prather[5], David Stevenson[2].

[1]CICERO Center for International Climate Research, Oslo, Norway
[2]School of Geosciences, University of Edinburgh, Edinburgh, UK
[3]Laboratoire des Sciences du Climat et de l'Environnement (LSCE), CEA-CNRS-UVSQ, Université Paris-Saclay, Gif-sur-Yvette, France
[4]Geophysical Fluid Dynamics Laboratory, National Oceanic & Atmospheric Administration, Princeton, NJ, USA
[5]Earth System Science Department, University of California Irvine, Irvine, CA, USA

Correspondence to: Srinath Krishnan (Srinath.krishnan@cicero.oslo.no)

Abstract.

Understanding the global hydrogen (H_2) budget is critical as H_2 is expected to play an important role in future energy systems. Tropospheric H_2 sources include direct emissions and atmospheric production via chemical reactions, while sinks are soil uptake and removal by hydroxyl radical (OH). Large uncertainties remain in quantifying the atmospheric production and loss of H_2 largely due to the lack of global-scale knowledge of the abundance of OH.

We use a suite of global three-dimensional Atmospheric Chemistry Models to evaluate key reactive species involved in atmospheric production and loss - formaldehyde (HCHO), nitrogen dioxide (NO_2), and carbon monoxide (CO) - with satellite retrievals. A box model is then used to simulate the evolution of global mean tropospheric H_2 from pre-industrial to present day; to test different relative contributions in atmospheric production from methane and Volatile Organic Compounds; and to assess atmospheric loss with different OH concentrations. Isotopic compositions are further used to constrain these sources and sink terms and assess the possibility of geological sources.

Models generally match satellite retrievals for HCHO, though model diversity exists for NO_2 and CO. From model evaluations and box model constraints, we estimate atmospheric H_2 production of 37-60 Tg/year, and atmospheric losses of 15-30 Tg/year, suggesting that some top-down literature estimates may overestimate production. Box model results suggest an upper bound 9 Tg/year for geological sources, considerably lower than the 23 Tg/yr proposed previously. We recommend more isotopic observations and targeted measurement campaigns to further refine the budget.

https://doi.org/10.5194/egusphere-2025-4898
Preprint. Discussion started: 29 October 2025

1 Introduction

A recently recalibrated H_2 observational dataset published by the NOAA Global Monitoring Laboratory showed that the globally averaged tropospheric mole fraction today is ~530 ppb, with an increase of 10 ppb over the last decade (Paulot et al., 2024; Pétron et al., 2024). This concentration varies spatially and seasonally because of changing sources and sinks for H_2. Estimates of the Global Warming Potential (GWP) of hydrogen depend on its atmospheric perturbation lifetime, highlighting the need to constrain its sources and sinks. The major H_2 source categories include atmospheric production from the oxidation of methane (CH_4, a volatile organic carbon, VOC) and non-methane VOCs (NMVOCs), as well as surface emissions from incomplete fossil fuel combustion, biomass burning, and nitrogen fixation from soils and oceans. Atmospheric production is estimated to account for up to 50% of the total sources, combustion for 30-40% and nitrogen fixation for 10-15% (Ehhalt and Rohrer, 2009).

In the atmosphere, H_2 is produced by photolysis of formaldehyde (HCHO), which is formed during the photochemical oxidation of methane with an estimated production range of 15-27 Tg/yr (Novelli et al., 1999; Paulot et al., 2024; Price et al., 2007; Sanderson et al., 2003). The oxidation of other VOCs, including biogenic VOCs also produces HCHO, contributing an additional 9-20 Tg/yr (Derwent and Jenkin, 2024; Novelli et al., 1999; Price et al., 2007). Estimates for atmospheric production using "top-down approaches" such as inverse modeling and seasonal isotopic compositions of H_2 generate much larger estimates for the total atmospheric production of 64-77 Tg/year (Rhee et al., 2006; Xiao et al., 2007) compared to "bottom-up approaches" where local measurements are upscaled to estimate global values (Hauglustaine and Ehhalt, 2002; Novelli et al., 1999; Pieterse et al., 2013; Price et al., 2007). Fossil fuel combustion sources represent hydrogen emissions from technological or man-made sources – 80% of which come from automobile traffic – and releases about 11-20 Tg/yr (Duncan et al., 2007; Ehhalt and Rohrer, 2009). H_2 emissions from biomass burning vary based on biomass type and burn conditions, with global estimates ranging from 8-20 Tg/yr (Andreae and Merlet, 2001; Ehhalt and Rohrer, 2009; Paulot et al., 2024). During nitrogen fixation, H_2 is produced as a by-product during the reduction of nitrogen (N_2) to ammonia (NH_3) by bacteria. While some of this H_2 is recycled, much of it escapes into the atmosphere (Conrad and Seiler, 1980). Global estimates for the H_2 released during N_2 fixation range from 6-12 Tg/year (Price et al., 2007; Rhee et al., 2006; Ehhalt and Rohrer, 2009). Other sources of hydrogen include fermentation, reaction of excited O atoms produced during O_3 photolysis with water molecules, aldehyde photochemistry, photolysis of glyoxal, and increased use of hydrogen in the energy sector which all contribute individually ~1 Tg/year of H_2 (Conrad and Babbel, 1989; Ehhalt and Rohrer, 2009; Pérez-Peña et al., 2022; Zimmerman et al., 1982). Leakages of hydrogen from industries or the energy sector are very uncertain but recent estimates suggest 1-2 Tg/yr (Esquivel-Elizondo et al., 2023; Trapani et al., 2025). Additionally, a recent study also suggests potential geological sources that can contribute as much as ~2 Tg/year (Zgonnik, 2020).

The two large sinks of hydrogen are the oxidation of H_2 by OH (15-23 Tg/year) (Ehhalt and Rohrer, 2009; Hauglustaine and Ehhalt, 2002; Paulot et al., 2021; Pieterse et al., 2013; Price et al., 2007) and soil uptake (53-88 Tg/year) (Ehhalt and Rohrer, 2009; Pieterse et al., 2011, 2013; Price et al., 2007; Rhee et al., 2006; Sanderson et al., 2003; Xiao et al., 2007; Yver et al.,

https://doi.org/10.5194/egusphere-2025-4898
Preprint. Discussion started: 29 October 2025

2011). During soil uptake, the removal of H_2 by soil bacteria is temperature- and moisture-dependent and is mediated through the enzyme activity of soil hydrogenase (Buzzard et al., 2022; Conrad, 1996). The large range in the soil sink reflects the bottom-up and the top-down approaches used to estimate the sink strength.

Isotopic studies complement H_2 budget evaluations as each of the sources and sinks have distinct isotopic values, and substantially different kinetic isotopic effects, respectively (Gerst and Quay, 2001; Pieterse et al., 2009; Rhee et al., 2006). The Deuterium/Hydrogen (D/H) isotopic ratios are expressed as $\delta D = (R_{SAMPLE}/R_{SMOW}-1)\times 1000$ (‰), where R_{SAMPLE} is the D/H ratio of sample and R_{SMOW} is that of Standard Mean Ocean Water (SMOW) (=0.015576±0.000006; Hagemann et al., 1970). Global mean δD of atmospheric H_2 has been observed to be 130‰ with several measurement campaigns being undertaken to measure isotopic values of the sources and fractionation during soil uptake (Batenburg et al., 2011; Gerst and Quay, 2001; Price et al., 2007). These include anthropogenic sources (Vollmer et al., 2010), biomass burning (Röckmann et al., 2010), N_2 fixation (Walter et al., 2012), photochemical oxidation (Rhee et al., 2008; Rice and Quay, 2009), and soil sinks (Rhee et al., 2006). A recent compilation of hydrogen isotopic values produced through different techniques/production means confirm that the isotopic values of produced H_2 carry the fingerprint of origin (Gibson et al., 2024). Studies such (Pieterse et al., 2011, 2013) have incorporated hydrogen isotopic calculations into the chemical mechanisms in TM5 (a 3-D ACM) and refined the H_2 budget. Isotopic values provide independent constraints on the H_2 sources and sinks, and, when combined with hydrogen concentrations can help constrain the atmospheric H_2 budget.

Atmospheric production and loss of H_2 depend on the availability and reactivity of the constituent species and their interactions with each other. Photochemical oxidation of CH_4 begins with the reaction with OH (rate-limiting reaction R1) and is followed by a chain of reactions that lead to formaldehyde (HCHO), a fraction of which then photolyzes to generate tropospheric H_2 (R2). Oxidation of NMVOCs also leads to HCHO, although with a more complex chain of reactions (not shown).

$$CH_4 + OH \rightarrow CH_3 + H_2O \quad \text{(R1)}$$

$$HCHO + h\vartheta \rightarrow H_2 + CO \quad \text{(R2)}$$

The production of tropospheric H_2 from CH_4 or VOCs can be estimated as a function of CH_4 burden, VOC emissions, tropospheric OH concentrations, HCHO yield from oxidation reactions, and the fraction of HCHO that is converted to H_2. Testing the accuracy of estimates from H_2 production from OH reactions is difficult because of the lack of direct measurements of the OH concentrations (Prinn et al., 1995), especially on a global scale (Yang et al., 2025). Atmospheric Chemistry Models (ACMs) that can simulate these chemical reactions provide an alternative tool to test our understanding of these reactions.

For the H_2 budget, atmospheric production and loss terms can be assessed by comparing intermediate species in the reaction pathways and chemical species that affect OH. Formaldehyde (HCHO) is a key intermediate pathway during the oxidation of CH_4 and VOCs and a relatively long record of satellite retrievals of tropospheric column HCHO is available (Chance et al., 2000; De Smedt et al., 2008). While not a direct proxy, the tropospheric OH concentration, important for atmospheric loss, is

https://doi.org/10.5194/egusphere-2025-4898
Preprint. Discussion started: 29 October 2025

sensitive to nitrogen oxides (NOx) and carbon monoxide (CO) concentrations (Dalsøren et al., 2016) – which have global satellite retrievals.

One significant drawback of ACMs is the substantial computing time and resources required for simulations. We have developed a box model based on results from the 3-D models in Sand et al. (2023) to calculate changes in H_2 concentrations with different budget terms. We have also integrated an isotopic module into the box model to calculate the isotopic composition of tropospheric H_2 (δD) in addition to concentration. This provides a way to evaluate ACMs that do not include isotopic coupling.

This study is structured as follows: we first investigate the atmospheric production and loss terms in the budget by comparing HCHO, NO_2 and CO in the ACMs used in Sand et al. (2023) against surface and satellite retrievals. Then, we use a box model to evaluate the temporal evolution of H_2 from pre-industrial to today. Additional simulations with the box model are conducted to evaluate the impact of varying the split between CH_4 and VOCs for atmospheric production, as well as the impact of different OH concentrations on atmospheric loss. As the soil sink term in the ACMs is tuned to reproduce reasonable H_2 concentrations, this study focuses on the chemical production and loss terms. Finally, we combine isotopic values and H_2 concentrations to constrain the contributions of atmospheric production and loss processes to tropospheric H_2 and explore the feasibility of having additional geological sources. Collectively, these approaches help refine the ranges for atmospheric terms and improve our understanding of the budget.

2 Methods

2.1 Multi-model chemistry evaluation

Here, we use the control simulations presented in Sand et al. (2023) for five models - OsloCTM3, UCI CTM, UKCA, LMDZ-INCA and GFDL-AM4.1. For WACCM6, we use a more recent simulation that is set up as the CTRL simulation described in Sand et al. (2023), except that it is run using CESM v. 2.1.2 and with 70 vertical levels (instead of 88 in Sand et al. 2023). All simulations use present-day atmospheric compositions and fixed hydrogen and methane surface concentrations. Further details on the models are provided in Table 1 and Sand et al. (2023).

Monthly model output for HCHO, OH, NO_2 and NO are used to calculate annual averages. Monthly-averaged satellite data for 2010 are downloaded for TROPOMI (Veefkind et al., 2012). The TROPOMI satellite has a global daily coverage and observes multiple atmospheric trace gas components O_3, NO_2, and HCHO with a spatial resolution of 5.5 km × 3.5 km and an equator crossing time at about 13:30 local time. Column-averaged tropospheric values are post-processed to calculate annual averaged values for HCHO, NO_2, and CO (no averaging kernels are applied to the retrievals; vertical profiles are shown in Fig. A1, A2). Similarly, MOPITT data for CO (Deeter et al., 2003) are compared to model results. This analysis is limited by the mismatch that arises due to the comparison of the monthly mean model outputs with satellite retrievals taken at a specific overpass time. To test how much this discrepancy can affect our comparison, we run an additional OsloCTM3 simulation for a year where the three hourly outputs are used.

https://doi.org/10.5194/egusphere-2025-4898
Preprint. Discussion started: 29 October 2025

130

Table 1: Details of the six models used here and Sand et al. (2023).

Model	Horizontal Res.	Vertical Res. (levels)	Meteorology	Chemistry	Dry deposition Parameterization	Simulation Length (time period averaged; years)	References
GFDL-AM4.1	~100kms	49	Wind speeds nudged to NCEP (6-hourly)	Tropospheric and stratospheric chemistry	Two-layer model; more details in (Paulot et al., 2021)	20 (10)	Dunne et al., 2020; Horowitz et al., 2020
LMDZ-INCA	1.25° x 2. 5°	39	ECMWF ERA5	State of the art tropospheric + stratospheric photochemistry	Seasonally and geographically varying dry deposition velocities	20 (3)	Hauglustaine et al., 2004
OsloCTM3	~2.25° x 2.25°	60	ECMWF 3-hourly open IFS	Tropospheric and stratospheric chemistry with 174 components and complex set of bi-molecular, tri-molecular, and heterogenous reactions.	Based on Sanderson (2003) scheme and (Price et al., 2007). More details in Sand et al. (2023)	20 (1)	Søvde et al, 2012
UCI CTM	T159L60N80 (~1.1 °)		ECMWF 3-hourly open IFS	Moderate tropospheric chem. with 30 species and 5-species in the stratosphere	Fixed deposition velocity	7 (1)	Prather et al., 2017
UKCA	~1.25° x 1.875°	85	Model's own	Full version of Chemistry with aerosol climatologies	Sanderson, 2003	14 (1)	Archibald et al., 2020
WACCM6	~1.875° x 2.5°	70	Model's own	Full tropospheric and stratospheric chemistry, with interactive oxidants and ozone	Computed within the land model	18 (5)	Gettelman et al., 2019

https://doi.org/10.5194/egusphere-2025-4898
Preprint. Discussion started: 29 October 2025

2.2 Description of the isotope-coupled box model

Running the 3-D ACM takes substantial computing resources, limiting its applicability in evaluating the relationship between the different budget terms and the atmospheric concentration of hydrogen. We use a box model that calculates the change in global atmospheric H_2 based on production and loss at every timestep (one month; equation 1)

$$\frac{dC}{dt} = Production - Loss = \frac{E + P_{atm}}{\beta} - C\frac{1}{\tau} \quad (1)$$

where C is concentration in ppb; dC/dt is change in concentration at every timestep; E corresponds to Emissions; P_{atm} is the atmospheric production of H_2; β is a factor used to convert from Tg to ppb; and $\frac{1}{\tau}$ represents the loss terms as a lifetime calculated by $\frac{1}{\tau} = \frac{1}{\tau_{OH}} + \frac{1}{\tau_{Soil}}$ where τ_{OH} and τ_{Soil} represent the lifetimes due to the OH radical and the soil-sink, respectively.

Emissions include time-varying emissions of H_2 from anthropogenic sources and biomass burning, and a constant natural source. Atmospheric production is calculated using time-varying methane concentrations and emissions of anthropogenic VOCs (including constant natural emissions). The two loss terms for atmospheric H_2 are represented by the soil-sink lifetime and the atmospheric lifetime.

A key aspect of this simple model is its flexibility, i.e. the model can be adapted to each atmospheric chemistry model. Atmospheric production, β-value (used to convert mass-values, which varies between models, to concentration), and the loss terms vary between the 3-D models and are tied to one another. The anthropogenic and biomass burning emissions for H_2 are adapted for each model. If available, model outputs are used for the split of H_2 atmospheric production from methane and NMVOCs, and natural emissions of NMVOCs. The sinks are determined by setting the atmospheric and soil uptake lifetimes.

We include a function in the box model to calculate the isotopic composition of atmospheric H_2. The different sources and sinks of hydrogen have distinct isotopic signatures. Combining the burden and the isotopic values, we use a mass-balance approach to calculate the isotopic values of tropospheric H_2 at every time step. This is compared with modern-day observation and acts as a two-pronged check on the total budget. Unless otherwise stated, we use isotopic compositions for sources and sinks from (Price et al., 2007) which are as follows: Anthropogenic emissions: -196‰; biomass burning: -290‰; atmospheric production (from CH_4 and NMVOCs): 162‰; Nitrogen fixation: -628‰ (Table 2). Fractionation factors of 0.943 and 0.58 are used for the soil-sink and OH loss, respectively. The box model does not account for the tropospheric-stratospheric H_2-cycling and the resulting tropospheric H_2-enrichment (Price et al., 2007; Pieterse et al., 2009). The stratospheric-tropospheric H_2 flux is not diagnostic output in the models considered in this study and remains uncertain. This omission can result in a 29-37‰ offset in δD.

https://doi.org/10.5194/egusphere-2025-4898
Preprint. Discussion started: 29 October 2025

3 Results

The results section is organized as follows: first, atmospheric production and loss of H_2 are assessed in the six models by comparing key species involved in these reactions with satellite retrievals. Next, the temporal evolution of H_2 concentrations from the pre-industrial to today is evaluated using the box model. Two specific cases related to atmospheric production and loss are analyzed. Finally, isotopic values are calculated in the box model to evaluate the overall tropospheric H_2 budget. Four scenarios are used to demonstrate how a dual constraint based on concentration and isotopic composition can help constrain the various sources and sinks.

3.1 Atmospheric Production

HCHO is a key intermediate species in the atmospheric production of tropospheric H_2. Through a series of complex, non-linear reactions, a substantial proportion of CH_4 and NMVOCs are oxidized to HCHO, some of which then photolyzes to produce H_2. Since the photolysis of HCHO is an important source of H_2, correctly capturing the background HCHO concentration is essential for constraining atmospheric H_2 production. A comparison with TROPOMI satellite retrievals shows that all models, except WACCM, produce reasonable formaldehyde concentrations, with global mean concentrations within 6.5% of the TROPOMI retrieval; Fig. 1, Fig. 2). However, there are notable regional differences: GFDL-AM4.1, LMDZ-INCA, and the UCI overestimate HCHO concentrations over South America, Africa, and parts of East Asia. Compared to TROPOMI, OsloCTM3 and UKCA exhibit lower concentrations over land, but higher over the oceans (Fig. 2). The WACCM model underestimates HCHO concentrations, particularly over land. The multi-model mean for HCHO matches well with the TROPOMI global mean, albeit affected by the lower values from WACCM. The consistent match between HCHO in the models and TROPOMI retrievals suggest that the 3-D models represent the production of atmospheric H_2 reasonably, since HCHO plays a crucial role in the reaction chain.

Additionally, we also compared model results against ATom measurement campaigns for nine different regions and four seasons (Figs. A1-A2). All models have comparably similar vertical profiles. They generally also match the ATom measurements other than in the W. Atlantic (A3) in the summer and autumn; and N. Pacific (P1) in the summer, and winter.

https://doi.org/10.5194/egusphere-2025-4898
Preprint. Discussion started: 29 October 2025

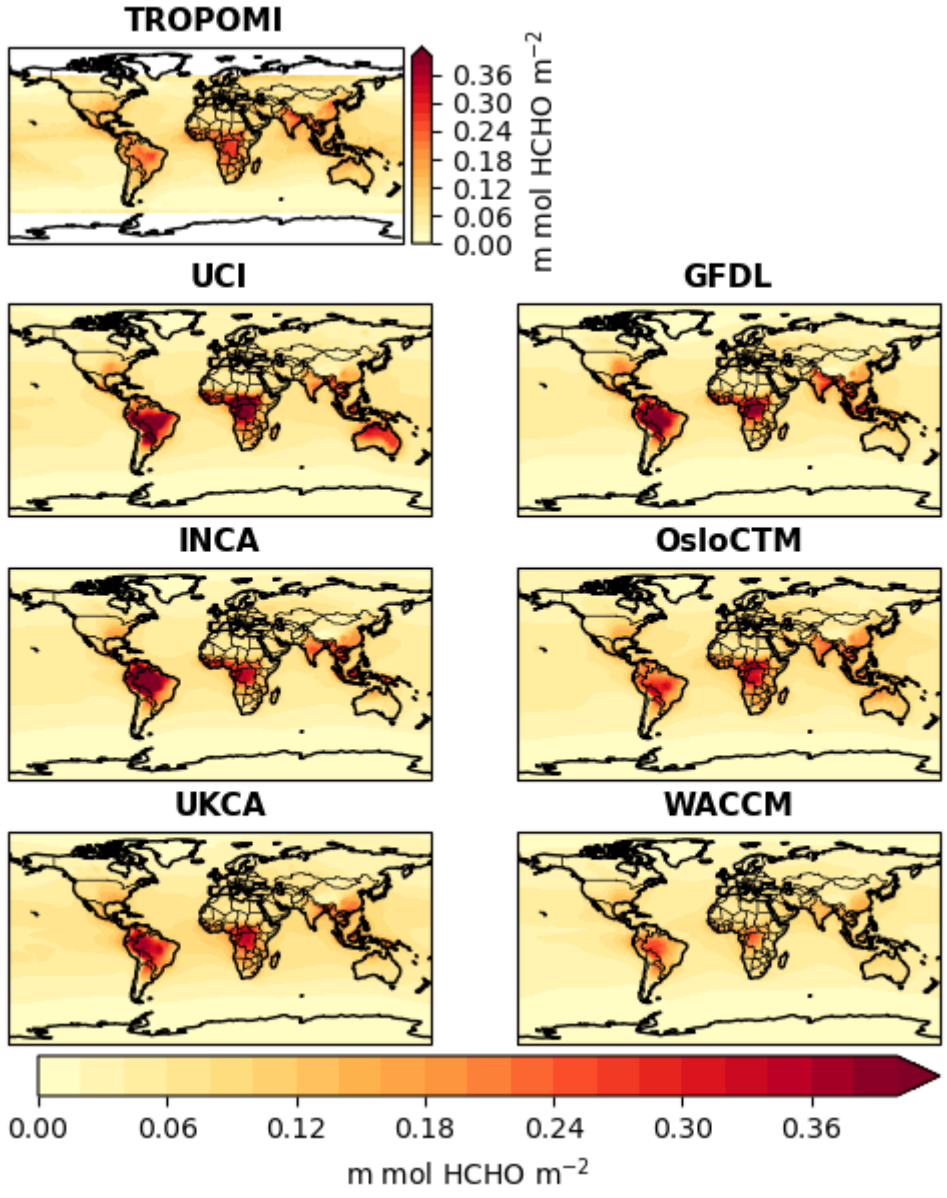

Figure 1: Spatial comparison of formaldehyde between TROPOMI satellite retrievals for 2010 and the different Atmospheric Chemistry Models listed in Table 1.

190

https://doi.org/10.5194/egusphere-2025-4898
Preprint. Discussion started: 29 October 2025

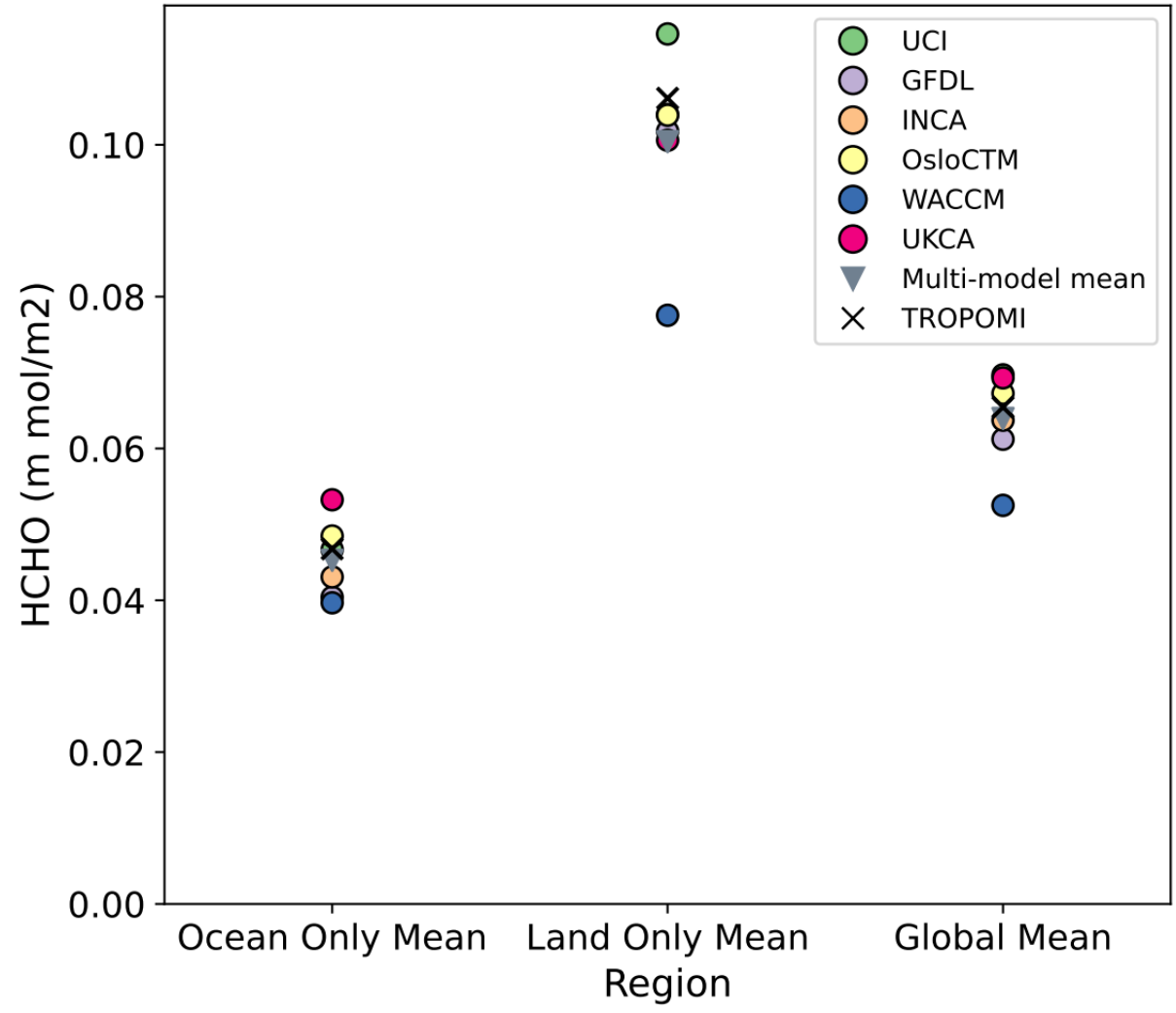

Figure 2: Comparison of annual mean formaldehyde over ocean, land, and global from TROPOMI satellite retrievals for 2010 (black crosses), six different ACMs (colored circles) and the multi-model mean (inverted triangle).

3.2 Atmospheric Production

195 The atmospheric loss of H_2 is primarily driven by its reaction with OH, a key oxidant in the atmosphere. Due to the short lifetime of OH (<1 second), direct retrievals of OH concentrations are not possible, therefore limiting a model-data comparison for OH. Indirect approaches, such as the use of a combination of carbon monoxide (CO) and NOx concentrations have been used to estimate OH levels for urban plumes and specific emission sources (Dalsøren et al., 2016; Lama et al., 2022). Although OH chemistry is influenced by several factors – such as photolysis reactions, temperature, 200 tropospheric ozone, humidity, methane and NMVOCs - NOx generally acts to increase OH concentrations and CO tends to reduce them.

https://doi.org/10.5194/egusphere-2025-4898
Preprint. Discussion started: 29 October 2025

In Fig. 3, we plot CO from the two satellite datasets, TROPOMI, MOPITT, and NO_2 from TROPOMI alongside model outputs for NO_2, CO, and OH. All models overestimate NO_2, with the global mean at least twice that of retrievals (Fig. 4). These differences are seen both over land and oceans (Fig. 3a and Fig. 4). This overestimation may result from comparing monthly mean outputs with satellite retrievals, which are restricted to specific overpass times and air mass factors. While we cannot replicate the specific air mass factors in OsloCTM3, if the mean calculations are restricted to specific satellite overpass times with the 3-hourly OsloCTM3 simulation, results show much lower values, bringing the model means closer to TROPOMI values and underestimating the values (Fig. 4a). The effect of using the ratio of NO_2 during overpass to the monthly mean for OsloCTM3 for the other models is shown in Fig. A3. For CO, there is general good agreement between the two satellite datasets (Fig. 3b). All the models underestimate CO, with large model-observation differences (10-20%) observed over the Northern Hemisphere mid and high latitudes. WACCM and OsloCTM3 have lower CO values compared to GFDL-AM4.1 and LMDZ-INCA models. All models also do a reasonable job of matching the vertical profiles of CO observed during the ATom campaign (supplementary). GFDL-AM4.1 and INCA have lower NO_2/CO ratio values compared to OsloCTM3, consistent with the elevated OH concentration in OsloCTM3 (Fig. 3c, d). Our results suggest that OH differences between models could be related to the local chemical environment (NOx/CO differences) with models showing a larger NO_2/CO ratio having larger OH values or vice versa. This could explain some of the diversity in atmospheric loss in the models.

https://doi.org/10.5194/egusphere-2025-4898
Preprint. Discussion started: 29 October 2025

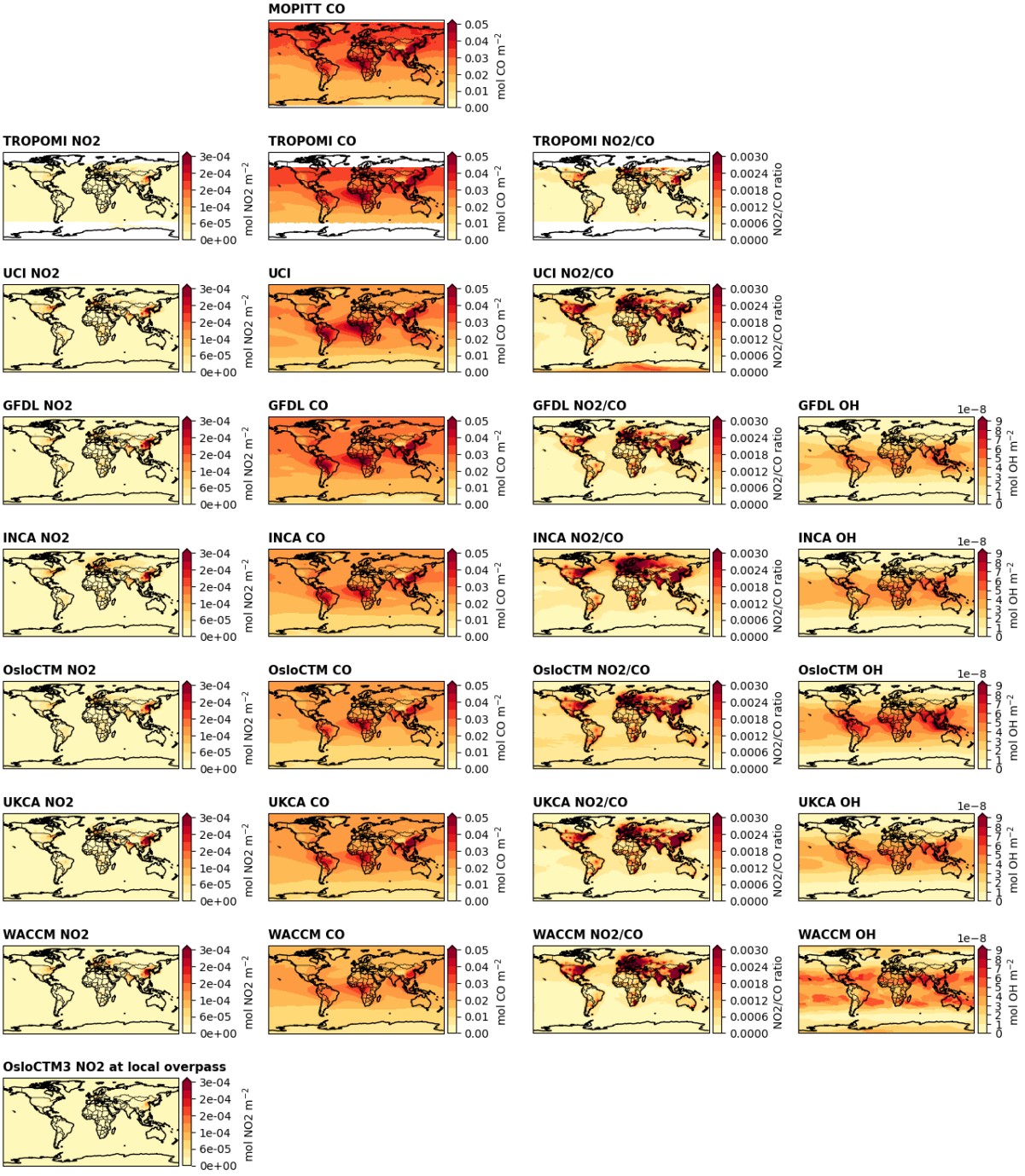

Figure 3: Global maps of annual mean satellite retrievals for (a) NO_2 for TROPOMI and models; (b) CO for MOPITT, TROPOMI and models; (c) NO_2/CO values in the models, and (d) OH in the models other than UCI.

https://doi.org/10.5194/egusphere-2025-4898
Preprint. Discussion started: 29 October 2025

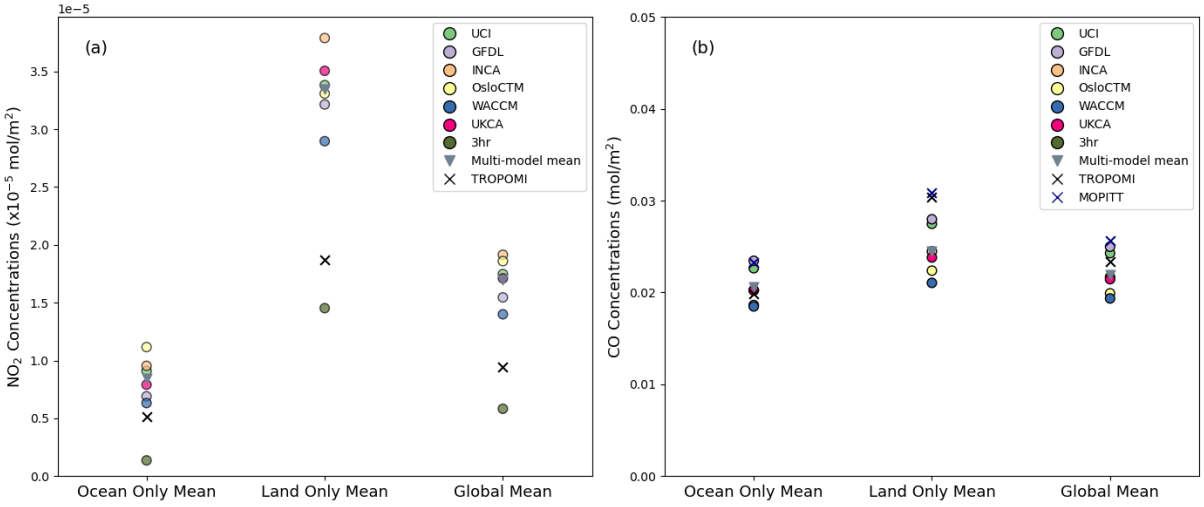

Figure 4: Comparison of annual mean (a) NO_2 and (b) CO concentrations over oceans, land, and global domains. Satellite retrievals from TROPOMI are shown as black crosses while MOPITT retrievals are represented by blue crosses. Colored circles denote results from the different ACMs, with the OsloCTM3 (3-hourly output) shown in dark olive green. The inverted triangle indicates the multi-model means calculated for model output with monthly means.

3.3 Box Model

In this study, 3-D model simulations have been conducted for the modern-day time slices. However, simulating the temporal evolution of tropospheric H_2 between the pre-industrial period and today using 3-D models is computationally very intensive and often prohibitive, making box models an attractive alternative (Fig. 5). The box model is initialized using an inferred pre-industrial H_2 concentration of 330 ppb (Patterson et al., 2020, 2021) and then model parameters adjusted to match the model results for the present-day OsloCTM3 simulations (Table A1). Panel (a) shows the evolution of the different emission and production terms of the budget in the box model, with anthropogenic emissions of H_2 scaled to CO emissions and atmospheric production following CH_4 concentrations showing a rise after the 1970s. Atmospheric H_2 production from NMVOCs also increases slowly post-1970s from ~20 Tg/yr to ~25 Tg/yr. Nitrogen fixation is set constant at 8 Tg/yr through the simulation and biomass burning emissions are set at 8 Tg/year till the 1990s, following which emissions are allowed to vary. Fig. 5b shows the split between total emissions and atmospheric production and 5c shows the resulting evolution of global mean tropospheric concentration of H_2. Crosses in Figs. 5b and 5c indicate H_2 concentrations from pre-industrial and present-day OsloCTM3 simulations. Although we do not compare box model results with observations, the crosses from the 3-D OsloCTM3 simulations agree well with the observed values.

https://doi.org/10.5194/egusphere-2025-4898
Preprint. Discussion started: 29 October 2025

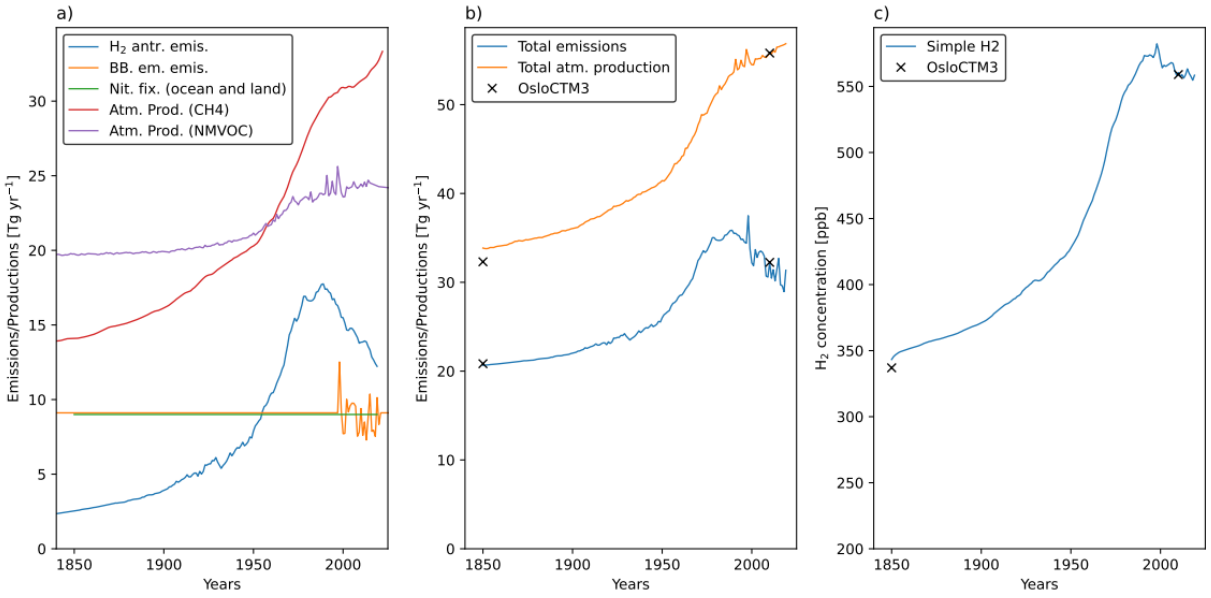

Figure 5: ***Temporal evolution of (a) emissions and atmospheric production; (b) total atmospheric production and total emissions; and (c) atmospheric concentration of H_2 from pre-industrial to today from the box model fitted to the OsloCTM3 model. The crosses indicate the pre-industrial value (1850) and the results from the OsloCTM3 modern day (2010).***

While the box model allows exploration of various uncertainties in H_2 evolution, such as the impacts of natural vs. anthropogenic emissions, different emission inventories, and the use of variable versus fixed soil-sinks - this study focuses on two specific issues related to atmospheric production and losses. A key question regarding atmospheric production is the significance of the relative contributions of H_2 production from CH_4 or NMVOCs. Total production is the sum of production from CH_4 and NMVOCs (not diagnosed in the ACMs), with the increase in production from CH_4 showing a larger increase over time. In the 1910s, a crossover occurs when production from CH_4 surpasses production by NMVOCs (Fig. 6a). The box model can be used to test the impacts of modifying this split (Fig. 6). In the control case, production from NMVOCs accounts for 44% of the total production (taken from the present-day OsloCTM3 3-D simulations) consistent with the estimate of Ehhalt and Rohrer (2009), while in the test case, this contribution is reduced to 39% following (Paulot et al., 2024). Consequently, pre-industrial H_2 production from NMVOCs decreases from ~20 Tg/yr to ~13 Tg/yr, while production from CH_4 increases from ~14 Tg/yr to ~18 Tg/yr (Fig. 6a). Total production in 1850 is reduced by ~4 Tg/yr with the gap narrowing over time until the 1980s, when both cases converge. The maximum difference in H_2 concentration between the two cases does not exceed ~15 ppb.

https://doi.org/10.5194/egusphere-2025-4898
Preprint. Discussion started: 29 October 2025

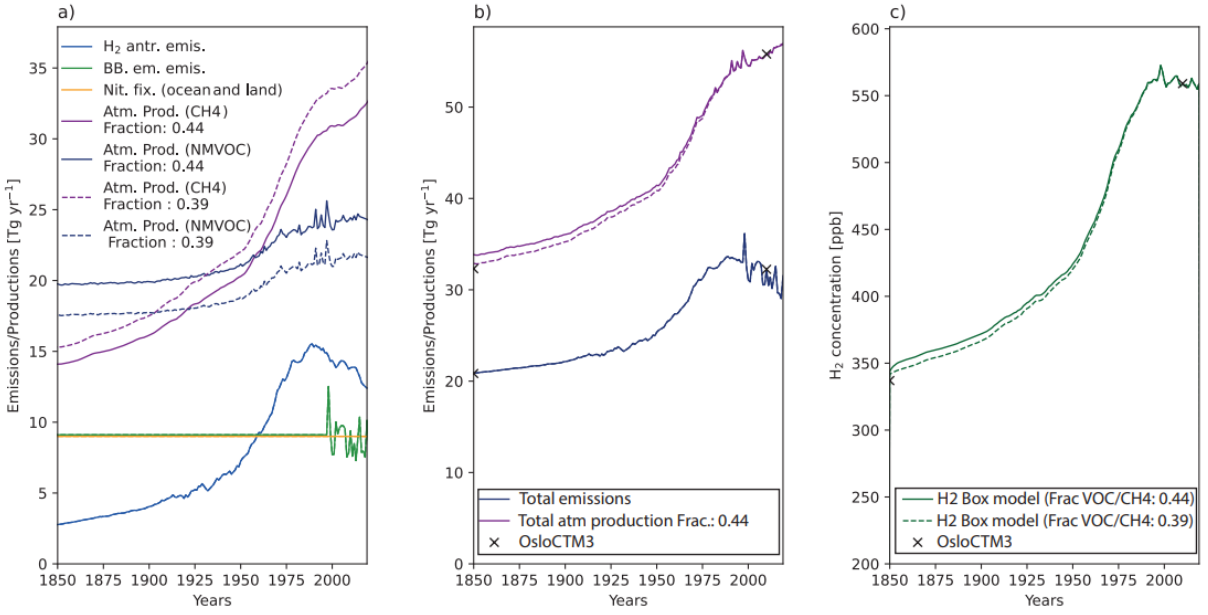

Figure 6: Similar to Fig. 5, but with different relative contributions of atmospheric production via CH_4 and VOCs. Solid lines represent values from a box model simulation with a VOC/CH_4 production ratio of 0.44 from Ehhalt and Rohrer, (2009), while stippled lines indicate results from a box model simulations with the ratio of 0.39 from (Paulot et al., 2024).

In the box model, atmospheric losses are defined by their lifetime, which depend on OH concentrations. We assess the effect of different lifetimes due to OH concentrations on tropospheric H_2, by running the model with three different atmospheric lifetimes that correspond to: (1) constant OH concentrations from pre-industrial to today; (2) pre-calculated OH concentrations by combining historical trends from Stevenson et al. (2020) with modern-day estimates from Skeie et al. (2023); and (3) using a scheme from the Third Assessment Report (TAR) where the OH-sink lifetime is adjusted following (Ehhalt et al., 2001; Table 4.11, footnote b) based on CH_4 concentrations, and emissions of CO, NOx, and VOCs (Fig. 7). Note that the OH concentrations here only affect the losses/sink term and not atmospheric production. These results indicate that using constant versus pre-determined OH-sink lifetimes produce similar H_2 concentrations through time. In contrast, applying the TAR scheme leads to higher H_2 concentrations, ~40 ppb greater than the other cases until the early 1970s – a couple of decades after the increase in anthropogenic emissions and a few years after the crossover point when atmospheric production from CH_4 dominates over production from NMVOCs. After the 1970s, the H_2 concentration from the three cases generally match each other. Results indicate that the various assumptions in the box model for the split between H_2 production from NMVOCs and CH_4 and for the time evolution of the atmospheric lifetime, which are not provided by the ACMs, have only a small effect on the H_2 concentration over recent decades.

https://doi.org/10.5194/egusphere-2025-4898
Preprint. Discussion started: 29 October 2025

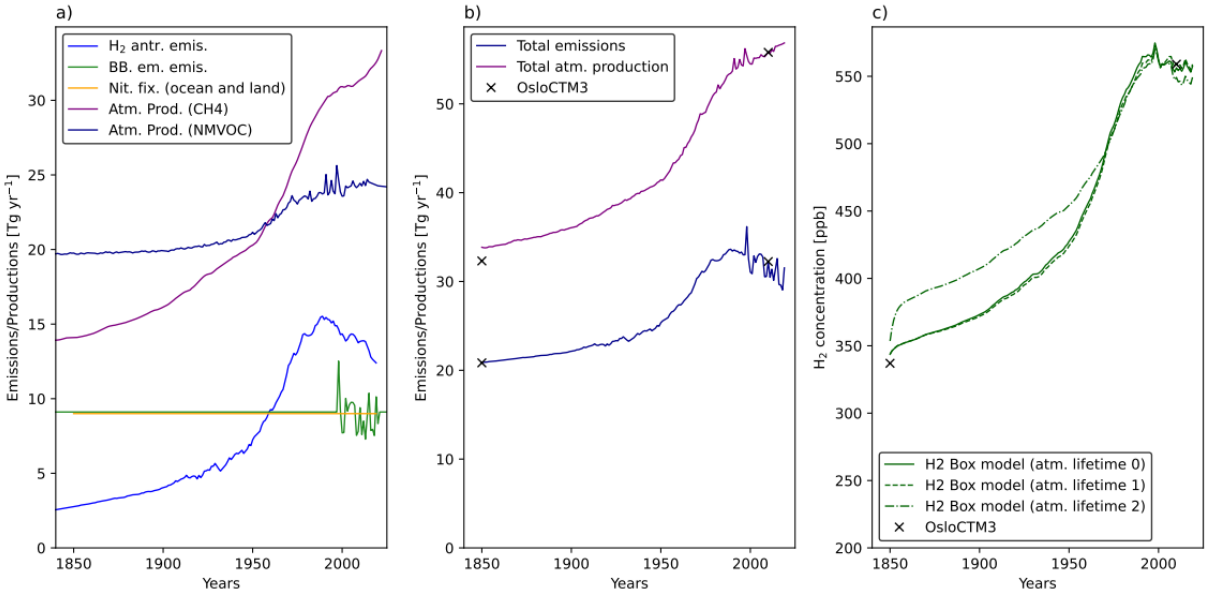

Figure 7: Similar to Fig. 5, but 7c shows the impact of having different atmospheric lifetimes due to different OH concentrations. The three OH-based lifetimes are calculated as Lifetime 0: Constant OH leading to constant atmospheric lifetime; Atm. Lifetime 1: Time-variant OH based on trends in Stevenson et al (2020) and Skeie et al (2023); Atm. Lifetime 3: time-variant OH using equations from the Third Assessment Report (Ehhalt et al., 2001).

3.4 Isotopic evaluations using the Box Model

In addition to H_2 concentrations, isotopic values of atmospheric H_2 are ~~also~~ calculated in the box model at every time step, depending on the relative contributions from the different sources and sinks. Fig. 8 shows the hydrogen atmospheric concentration vs. isotopic composition for the different box model simulations fit to match the ACMs and from published literature. All the models show a narrow range of atmospheric H_2 concentrations (520-540 ppb) and a wider range for isotopic values (20-210‰), with WACCM at the lower-end and UKCA at the higher-end. The low isotopic value in WACCM is due to the low atmospheric H_2 production resulting in more enriched H_2. The high value for isotopic composition in UKCA is due to high soil sink in UKCA, resulting in more depleted H_2. Published studies have ranges for both predicted H_2 and isotopic values of 365-550 ppb and 0-150‰ respectively. That the isotopic range is large is not surprising as most of these studies look at the concentration budget and not the isotopic budget. For example, Fig. A4 shows the resulting budgets if isotopic values and fractionation factors for the different sources and sinks are taken from (Pieterse et al., 2011) rather than (Price et al., 2007) (and not including the stratospheric exchange which will enrich all isotopic values). We present this spread here, not to evaluate them against models, but to reiterate the benefit of combining H_2 concentrations with δD to constrain the different budget terms.

https://doi.org/10.5194/egusphere-2025-4898
Preprint. Discussion started: 29 October 2025

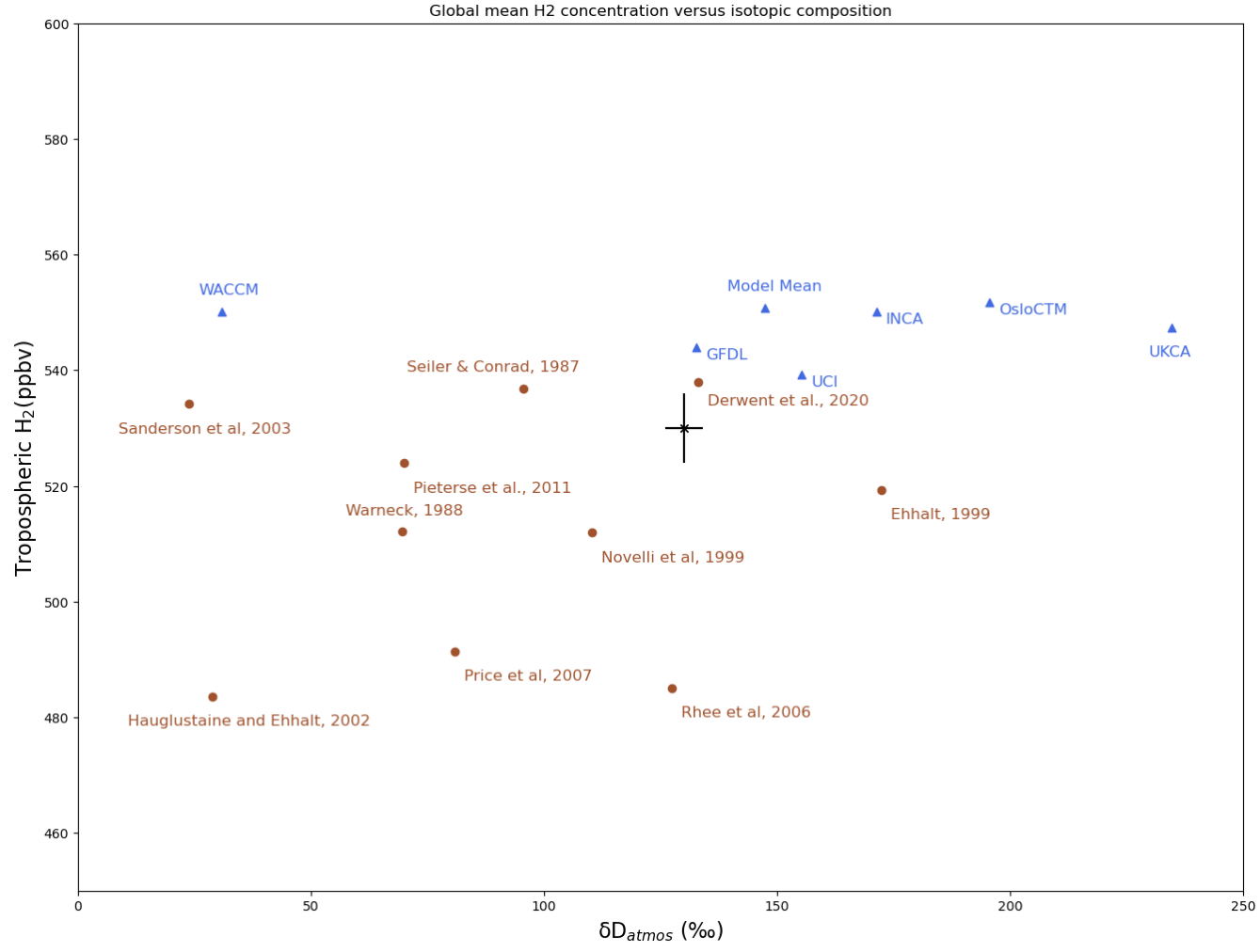

Figure 8: Relationship between atmospheric hydrogen mole fraction and isotopic composition (δD) from different models (triangles) and published literature (circles). The cross indicates the observed range of lower tropospheric H_2 concentrations between 1991-1996 of 531±6 ppb (Novelli et al., 1999) and δD values (Price et al., 2007; the sensitivity to using values from Pieterse et al., 2011 is shown in Fig. A4). The model concentrations are higher than observed possibly because they are calibrated for more recent observations. (Paulot et al., 2024) suggests an increasing trend of ~1.7ppb/year.

We present four cases where the sources and sinks are modified to demonstrate this approach (Fig. 9): (1) a base case using modern-day values; (2) high atmospheric production where atmospheric production values from a top-down estimate (Rhee et al., 2006) are used; (3) low atmospheric production and (4) additional geological source of 23 Tg/year as suggested by (Zgonnik, 2020). To balance the budget for H_2-concentrations, we adjusted the soil sink to account for the additional H_2 (Table 2). These cases are chosen to constrain the range of atmospheric production estimates and potential geological inputs by evaluating feasibility to fall within observed concentration and isotopic ranges. It should be noted that geological sources can span a wide range of isotopic values from 0 to -1000‰. We choose a value of -385‰ which is the mean of the white

https://doi.org/10.5194/egusphere-2025-4898
Preprint. Discussion started: 29 October 2025

hydrogen values suggested in Gibson et al. (2024). The effect of using a different isotopic value for a geological source is shown in Fig. A5.

Table 2: Values used for the emissions, isotopic values for the sources and lifetime and fractionation factors used for the four different cases in the box model.

Case	Anthropogenic emissions		Biomass Burning		Nitrogen Fixation		Atm. Production		Geological Sources		Atm. Loss		Soil Uptake	
	Emissions (Tg/yr)	δD (‰)	Emissions (Tg/yr)	δD (‰)	Emissions (Tg/yr)	δD (‰)	Emissions (Tg/yr)	δD (‰)	Emissions (Tg/yr)	δD (‰)	Lifetime (yrs)	Frac. Factor	Lifetime (yrs)	Frac. Factor
Base case	13.3	-196	13.3	-290	9	-628	46.9	162	0	-385	7.74	0.94	3.41	0.58
High atm. production	13.3	-196	13.3	-290	9	-628	77	162	0	-385	7.74	0.94	2.30	0.58
Low atm. production	13.3	-196	13.3	-290	9	-628	30	162	0	-385	7.74	0.94	3.41	0.58
Geological sources	13.3	-196	13.3	-290	9	-628	46.9	162	20	-385	7.74	0.94	3.00	0.58

https://doi.org/10.5194/egusphere-2025-4898
Preprint. Discussion started: 29 October 2025

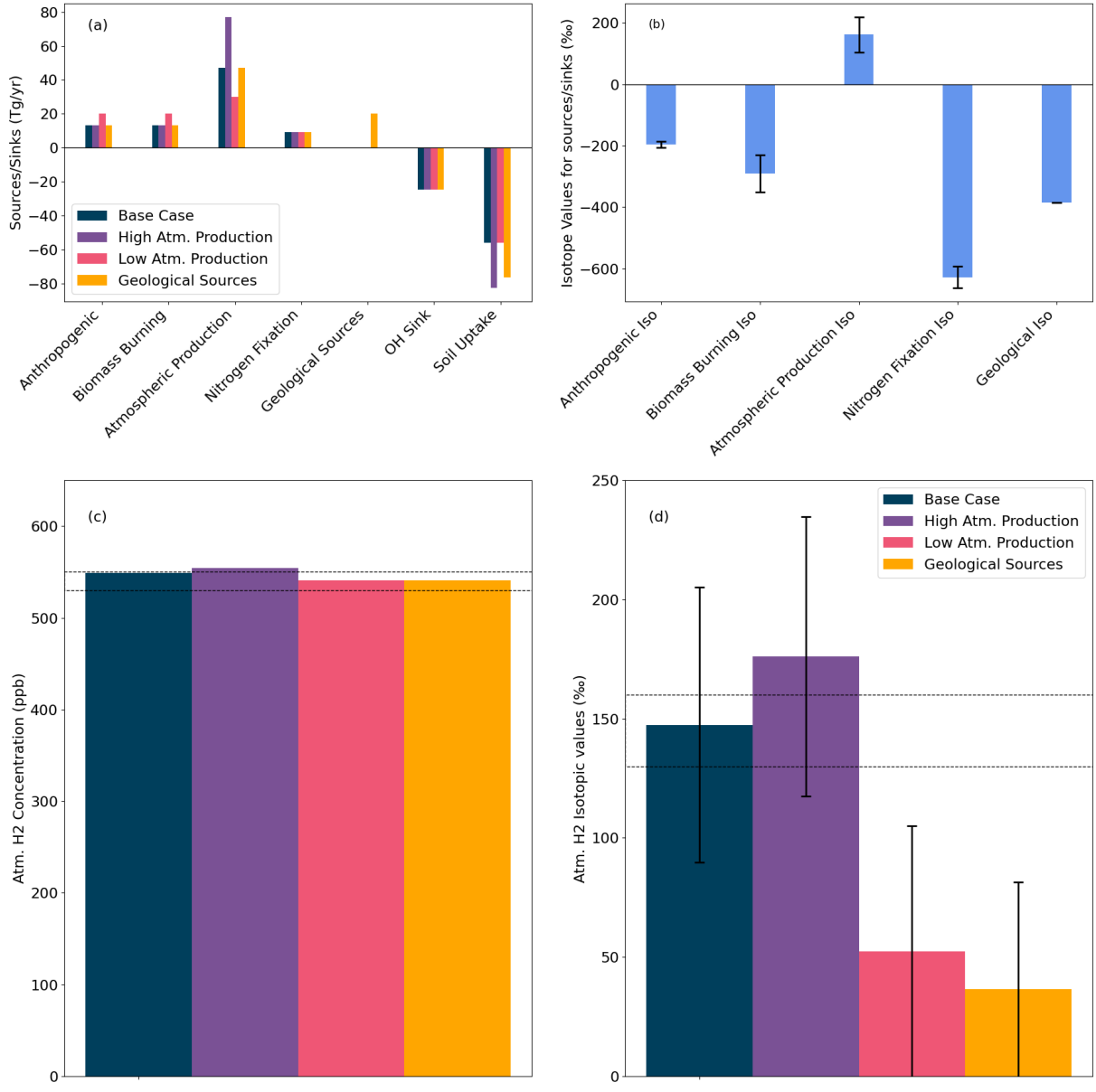

Figure 9: Box model results with isotopic calculations for the Base case (dark blue bars), high atmospheric production (purple), low atmospheric production (pink) and geological sources (yellow) (a) showing the burdens for different sources and sinks used in the box model; (b) isotopic values for the sources used in box model; (c) calculated H_2 concentration; and (d) calculated isotopic values for tropospheric H_2 for the different cases. The dashed black lines show the observed range in (c) H_2 concentration taken here as 530-550 ppb to account for changes in concentrations since Novelli et al. (1999) and (d) H_2 isotopic compositions from Gerst and Quay (2001).

Fig. 9a shows the magnitude of the different sources and sinks for hydrogen in the four cases and Fig. 10b shows the isotopic values for the sources used in the box model. The resulting hydrogen concentrations for the four cases are shown in Fig. 9c.

https://doi.org/10.5194/egusphere-2025-4898
Preprint. Discussion started: 29 October 2025

All four cases produce atmospheric concentrations that are broadly near the observed concentration range (in dashed lines). However, the corresponding isotopic compositions are much more sensitive compared to H_2 concentration and fall far outside the observed ranges (in this case taken as 530-550 ppb to account for an increase in H_2 concentrations since 1991-1996 and 130‰ - 160‰) for the three perturbed cases. This clearly indicates that low and high atmospheric production values do not agree with the observed H_2-isotopic values. Further, a geological source (with a corresponding increase in soil uptake) shows an even bigger shift in δD – not observed today.

Uncertainty ranges for the isotopic signatures of each source were used to calculate the maximum possible uncertainty. The most depleted and enriched source combinations were applied to calculate the minimum and maximum ranges shown in Fig. 9d. These results indicate that while high atmospheric production can be accommodated within the budget if extremely depleted isotopic values are used for the other sources, scenarios with lower atmospheric production and high geological sources do not fit the budget.

The influence of the individual sources and sinks on the final tropospheric mole fraction and isotopic composition of tropospheric H_2 is shown in Fig. 10 as the effect of a 2% change in the source or sink strength. Among the sources, atmospheric production has the largest effect on both the tropospheric H_2 and isotopic compositions, with each of the other sources having less than 1/3rd of the impact. The two sinks also play a huge role with the soil sink making the isotopic values more negative, while the OH sink shifting them to more positive values.

https://doi.org/10.5194/egusphere-2025-4898
Preprint. Discussion started: 29 October 2025

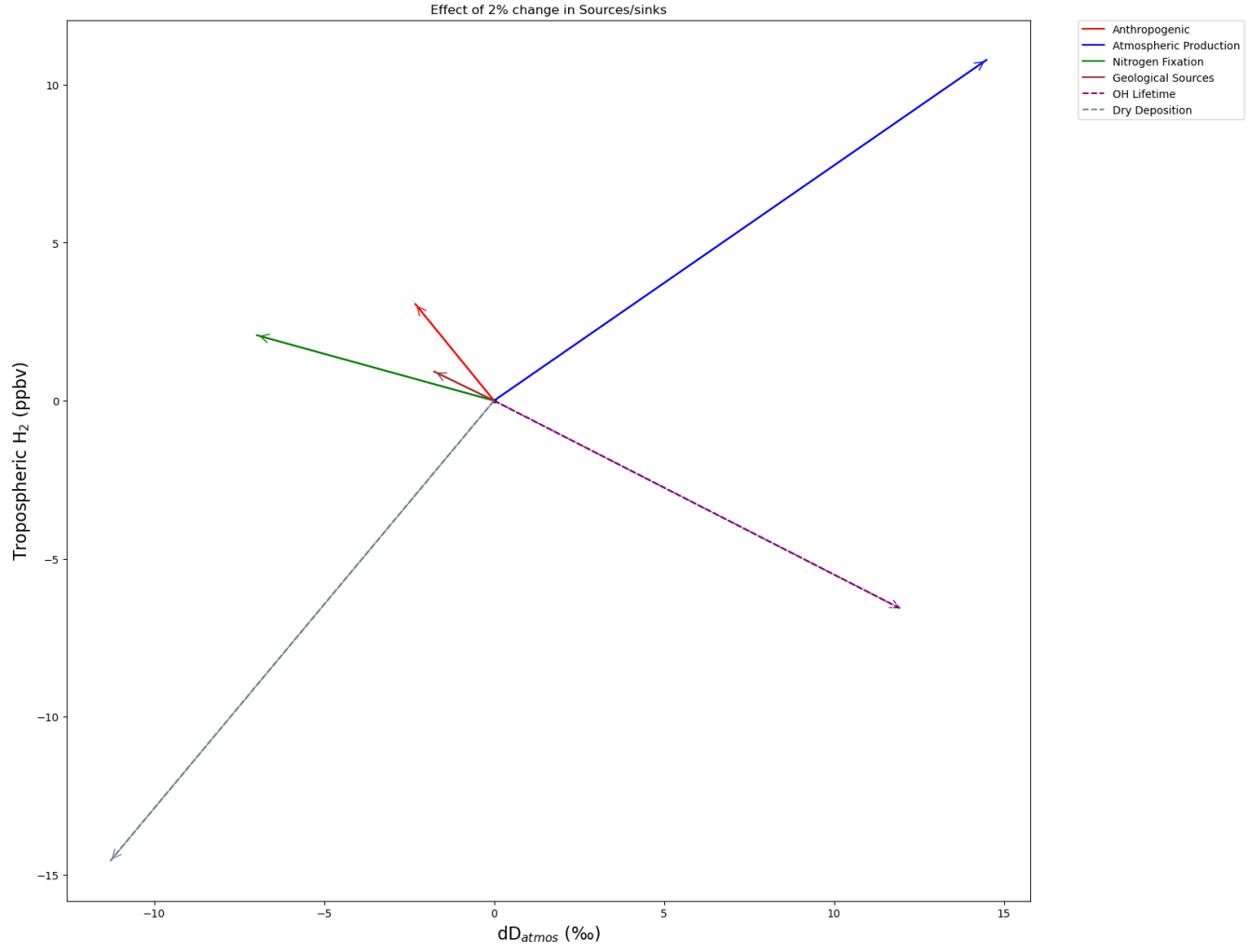

Figure 10: Impact of individual sources and sinks on the tropospheric mole fraction and the isotopic composition of H_2.

345

We extend this analysis by evaluating what adjustments to individual sources would be required to accommodate geological sources. While multiple source-sink combinations exist that fit within the concentration and isotopic constraints, we restrict this sensitivity analysis to emissions from anthropogenic sources, biomass burning, and nitrogen fixation. Based on model evaluations and box model constraints the atmospheric production and soil sink are allowed to vary between 37-60 Tg/yr and
350 49-77 Tg/yr respectively. The range for soil sink is derived by running the box model across the specified range of atmospheric production values to identify feasible soil sink estimates that satisfy the observed concentration and isotopic constraints for tropospheric H_2.

Table 3 shows the maximum geological source consistent with low, mid, and high estimates of the three sources. The results indicate that the maximum plausible geological source, given the constraints is 9 Tg/yr – if we are overestimating N_2 fixation

https://doi.org/10.5194/egusphere-2025-4898
Preprint. Discussion started: 29 October 2025

or biomass burning inputs. Thus an estimate of 23 Tg/yr as suggested by Zgonnik (2020) is not possible with our assumed isotopic composition of the geological input. However, greater contributions from isotopically enriched volcanic sources can affect this upper bound.

Table 3: Maximum allowable geological source input, constrained by adjusting emissions from anthropogenic, biomass burning, and nitrogen fixation within their respective observed low, mid, and high ranges.

Source Adjusted	Values (Tg/yr)	Maximum geological source possible (Tg/yr)
Anthropogenic	10	6
	13.3	4
	20	0
Biomass Burning	7	9
	13.3	4
	2	-
Nitrogen Fixation	6	9
	9	4
	12	-

4 Implications and conclusions

Chemical comparisons for atmospheric production and loss show that our models generally agree with satellite retrievals for HCHO, NO_2, and CO. Ranges for the different sources and sinks for the models and from published literature are shown in Fig. 11. All model values are below the two highest estimates of atmospheric production using the top-down estimates. Isotopic evaluations using the box model also show that these high values of atmospheric production lie outside the range of observed isotopic ranges (Fig. 9). These suggest that atmospheric production values lie within the range of 37-60 Tg/yr as shown in Fig. 11. Atmospheric loss in the models is higher than that observed in literature – possibly related to range in OH concentrations in the models (Yang et al., 2024). However, lacking OH observations and to balance the budget, we suggest a larger range for atmospheric loss of 15-30 Tg/yr. Soil sink estimates are constrained to 49-77 Tg/yr, given the new constrained range in atmospheric production.

https://doi.org/10.5194/egusphere-2025-4898
Preprint. Discussion started: 29 October 2025

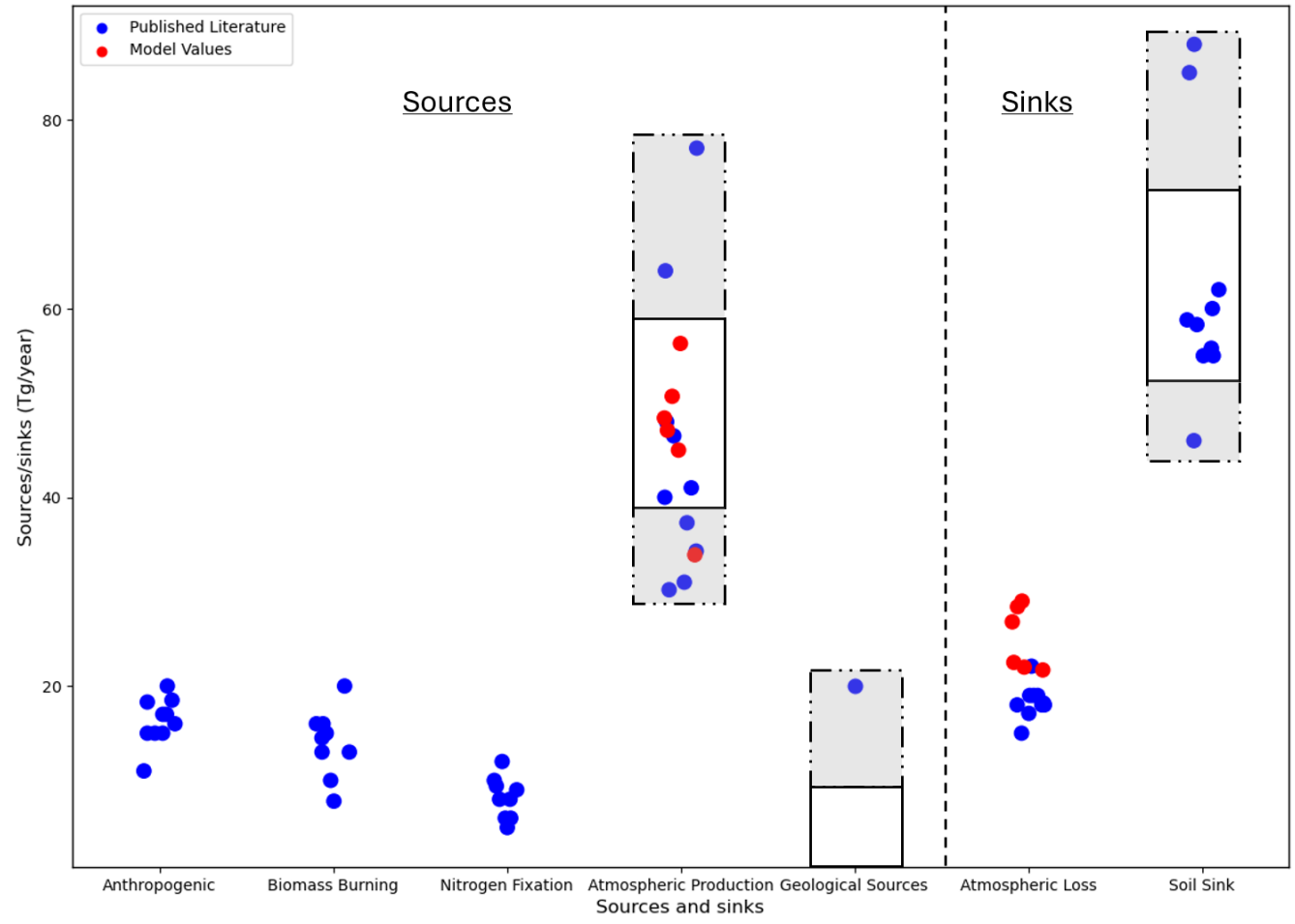

Figure 11: Sources and sinks in the tropospheric hydrogen budget, showing updated ranges for atmospheric production, atmospheric loss based on this study. The grey shaded area with dashed outlines represents previously reported ranges, while the solid white boxes indicate the updated ranges. Model values are shown for the atmospheric production and loss terms that are analyzed in this study.

This study is limited by the uncertainties associated with each budget term (both concentrations and isotopic values), whether from observational estimates or models. Using geological sources with isotopic values of -100‰ to 0‰, rather than -385‰ that we use, would allow for a larger geological input but it would still require a rearrangement of the other budget terms. Another source of uncertainty is the input from stratospheric-tropospheric exchange, which can cause an enrichment between 29‰ (Pieterse et al., 2011) to 37‰ (Price et al., 2007) or. As this exchange is not included in the box model, it is not accounted for in this study but needs further investigation in the future. (Pieterse et al., 2013) also found that dry deposition plays an important role in the isotopic budget. In this study, because the models have tuned the dry deposition

https://doi.org/10.5194/egusphere-2025-4898
Preprint. Discussion started: 29 October 2025

values to produce reasonable concentrations, we do not evaluate or change this term. Other potential additional validations of the budget, such as seasonal variations, recent trends and a more detailed analysis of the latitudinal variations of hydrogen are also beyond the scope of the current setup of the box model.

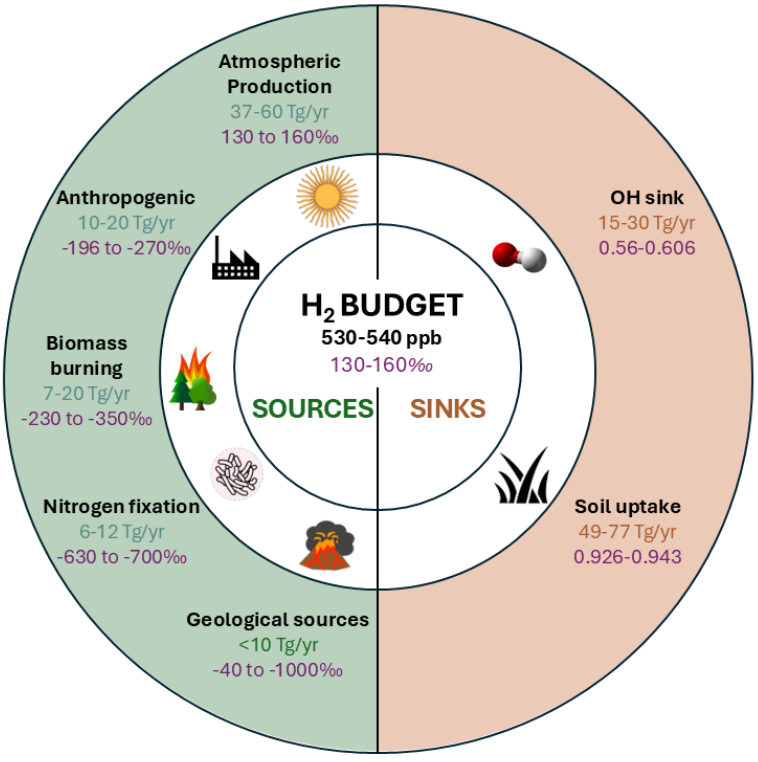

Figure 12: An updated estimate of source and sink ranges based on existing literature and this study. Numbers include the range of sources (green) and sinks (brown) in Tg/yr and isotopic values of sources and fractionation factors for the sinks (in purple).

Our results show that six different ACMs with different chemistry schemes show similar rates of HCHO tropospheric mole fraction – a proxy used here to evaluate atmospheric production and broadly match TROPOMI satellite retrievals. There is a larger diversity in OH indicating more uncertainty and a bigger spread for atmospheric losses. These could be related to different chemistry and different NOx/CO chemical environments in the models. We employ a box model to simulate the evolution of atmospheric H_2 from pre-industrial to today, exploring the impacts of having different CH_4/VOC relative contributions for atmospheric production and OH lifetimes for atmospheric losses. The ability of the box model to reproduce the broad trends in H_2-concentrations over time suggests that the budget terms reasonably represent the global H_2 cycle. Using combined constraints from atmospheric concentrations and isotopic values, the box model suggests atmospheric production to be in the range of 37-60 Tg/year. Photochemical losses are constrained to 15-30 Tg/year and soil sink is constrained to 49-77 Tg/yr (Fig. 12). These values are more consistent with the "bottom-up" estimates and reflect our current

https://doi.org/10.5194/egusphere-2025-4898
Preprint. Discussion started: 29 October 2025

understanding based on a combination of model analysis, and expert judgment. Our study highlights the critical need for more isotopic observations of atmospheric H_2 to refine our understanding of the hydrogen budget.

405

Appendices

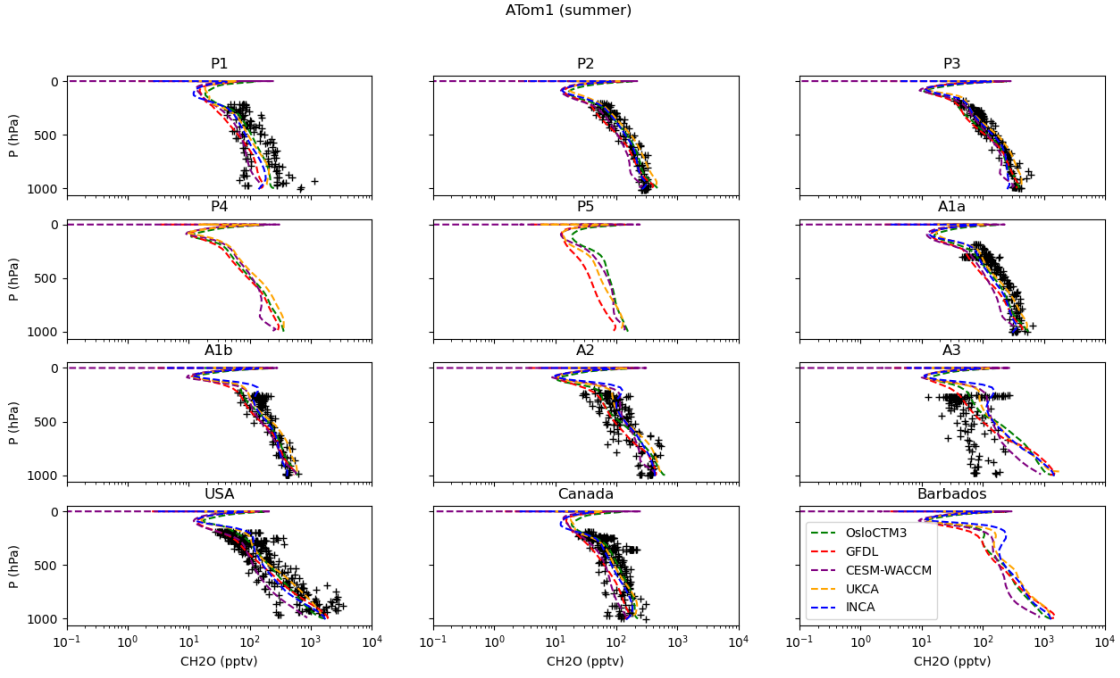

https://doi.org/10.5194/egusphere-2025-4898
Preprint. Discussion started: 29 October 2025

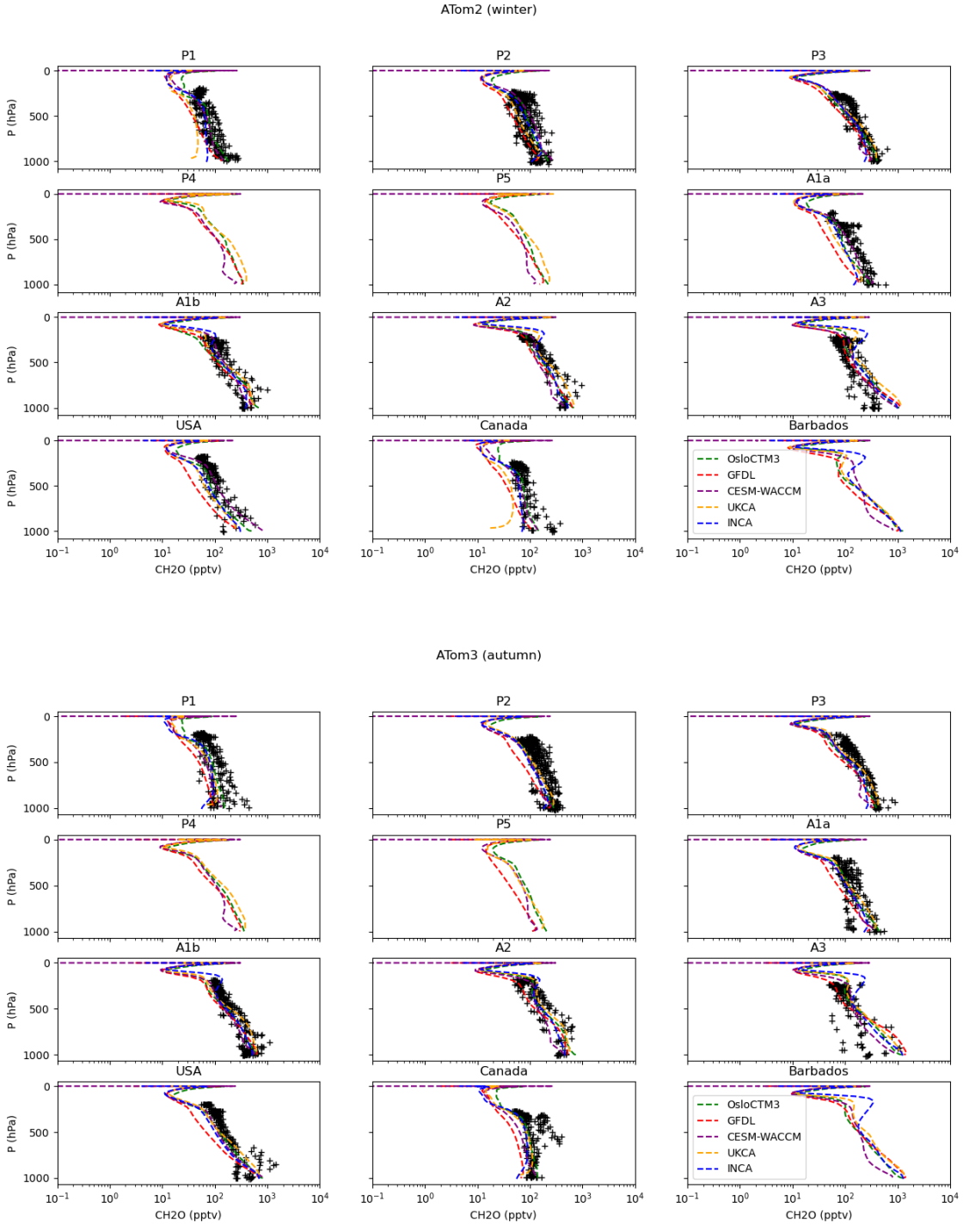

410

https://doi.org/10.5194/egusphere-2025-4898
Preprint. Discussion started: 29 October 2025

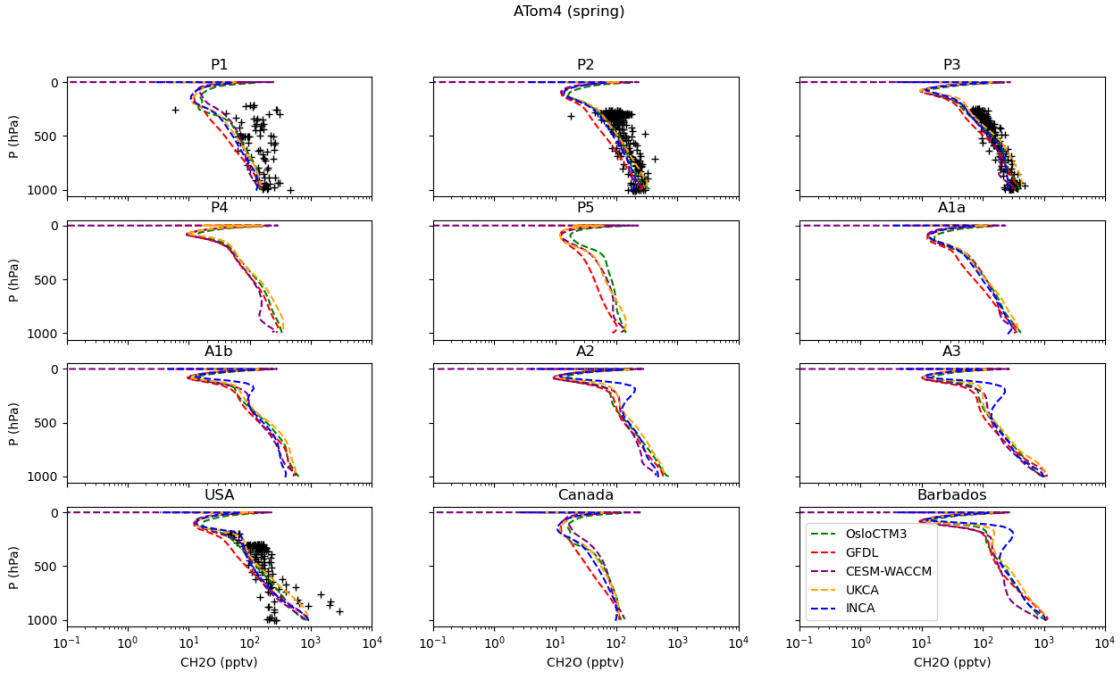

Figure A1: Vertical profiles of formaldehyde (HCHO) compared against observations from four different ATom campaigns. Each panel corresponds to a specific geographical box, defined by latitude and longitude bounds: P1 (180°W to 135°W, 60°N to 90°N): Polar North Pacific; P2 (180°W to 135°W, 30°N to 60°N): Mid-latitude North Pacific; P3 (180°W to 135°W, 0°N to 30°N): Equatorial North Pacific; P4 (160°E to 135°W, 30°S to 0°S): Equatorial South Pacific; P5 (160°E to 135°W, 60°S to 30°S): Mid-latitude South Pacific; A1a (45°W to 10°W, 30°N to 60°N): Mid-latitude North Atlantic; A1b (45°W to 10°W, 0°N to 30°N): Equatorial North Atlantic; A2 (45°W to 10°W, 30°S to 0°S): Equatorial South Atlantic; A3 (65°W to 30°W, 60°S to 30°N): Western Atlantic; USA (135°W to 80°W, 30°N to 60°N); Canada (135°W to 45°W, 60°N to 90°N); Barbados (80°W to 45°W, 0°N to 30°N).

https://doi.org/10.5194/egusphere-2025-4898
Preprint. Discussion started: 29 October 2025

420

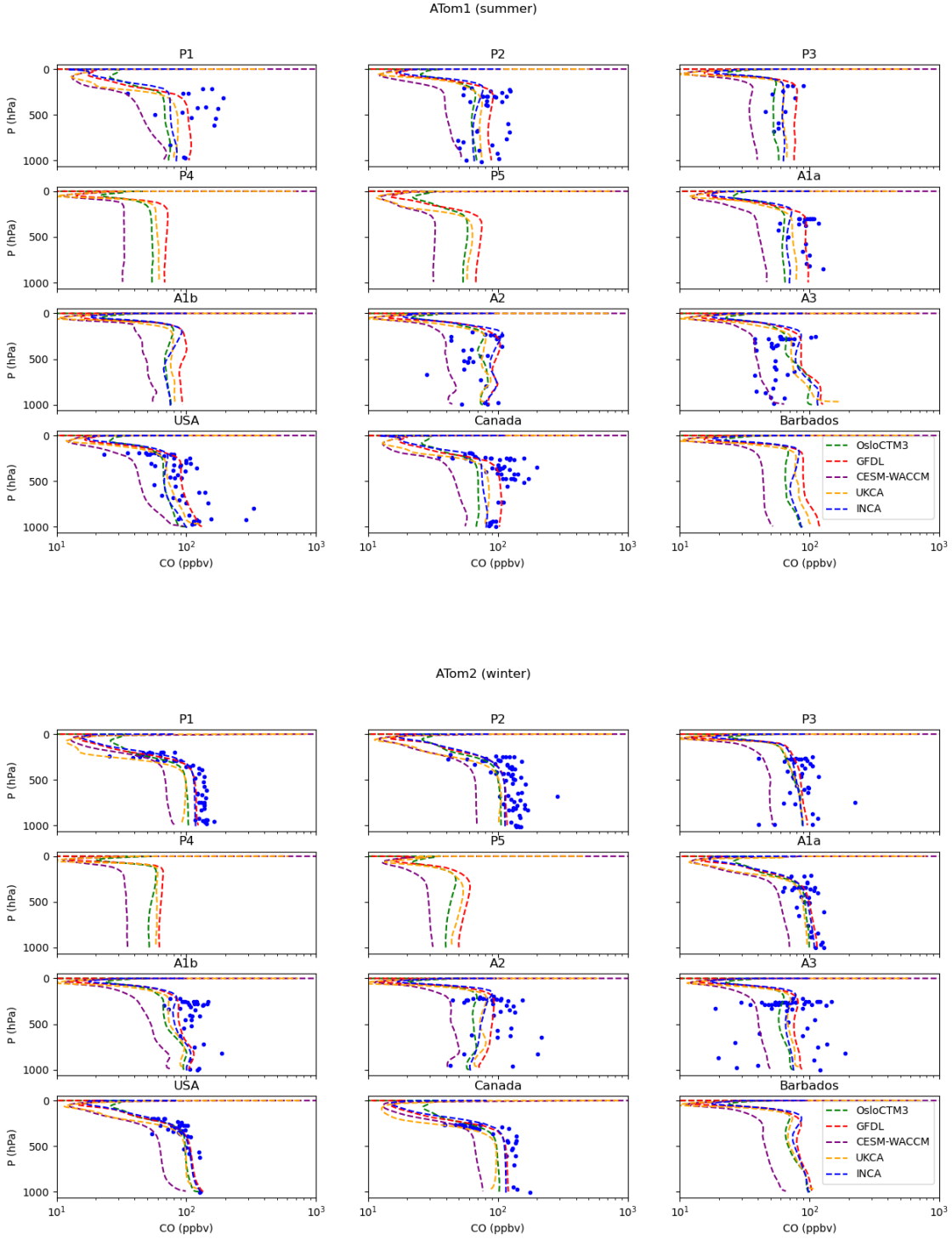

https://doi.org/10.5194/egusphere-2025-4898
Preprint. Discussion started: 29 October 2025

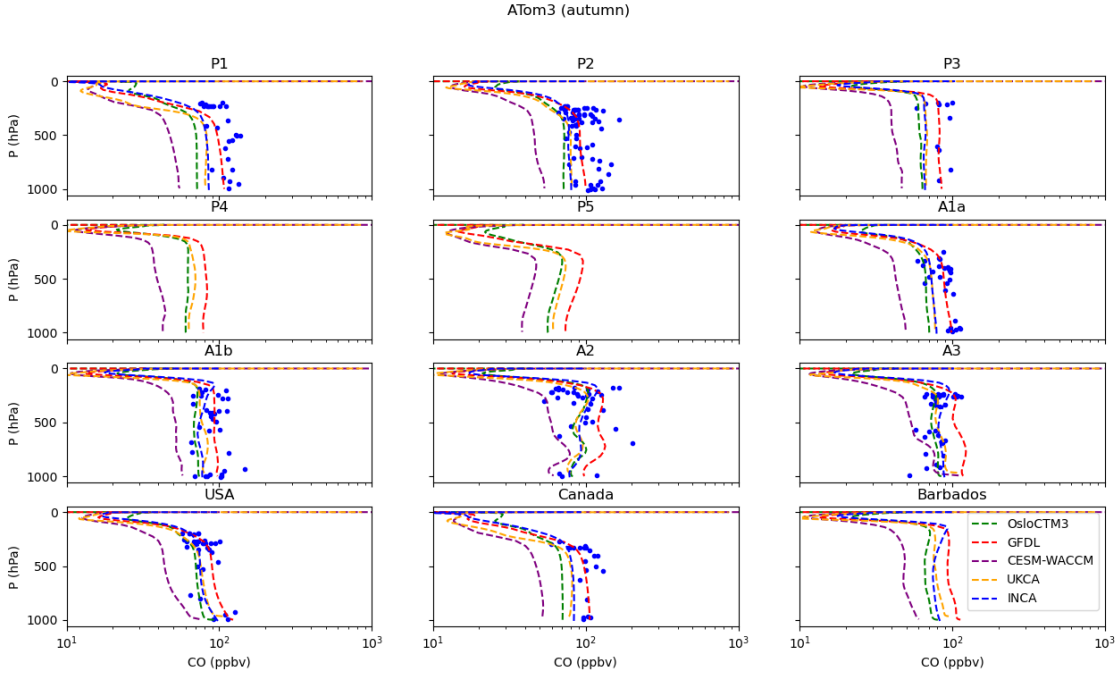

425

https://doi.org/10.5194/egusphere-2025-4898
Preprint. Discussion started: 29 October 2025

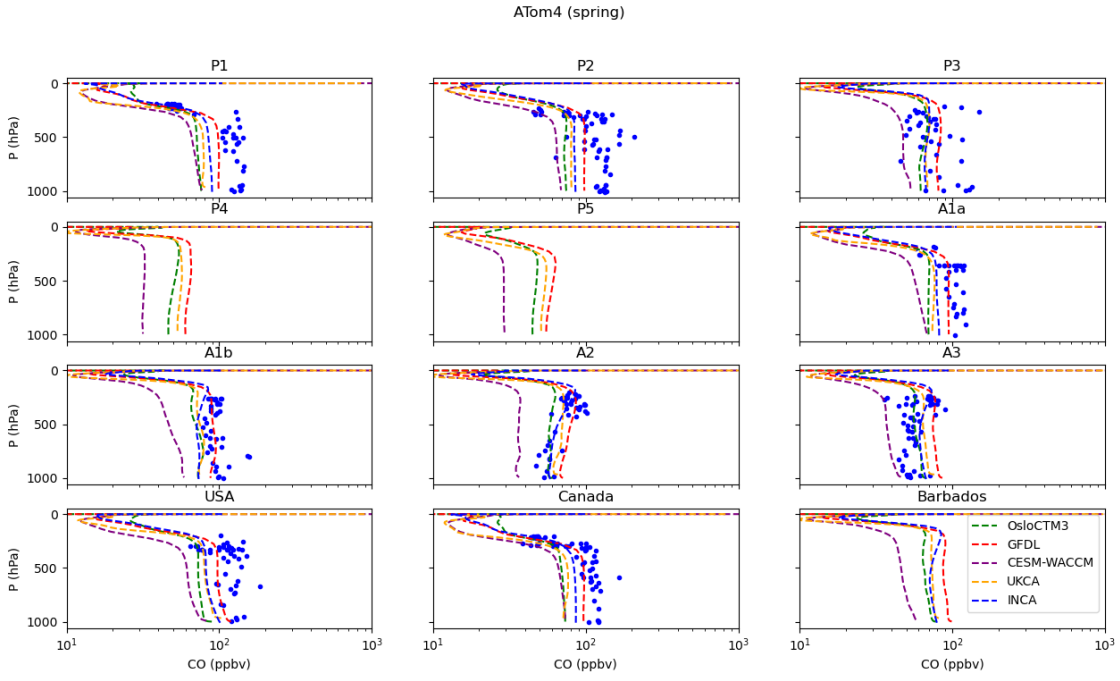

Figure A2: Similar to Fig. A1 but for vertical profiles of carbon monoxide against observations from the ATom campaigns.

https://doi.org/10.5194/egusphere-2025-4898
Preprint. Discussion started: 29 October 2025

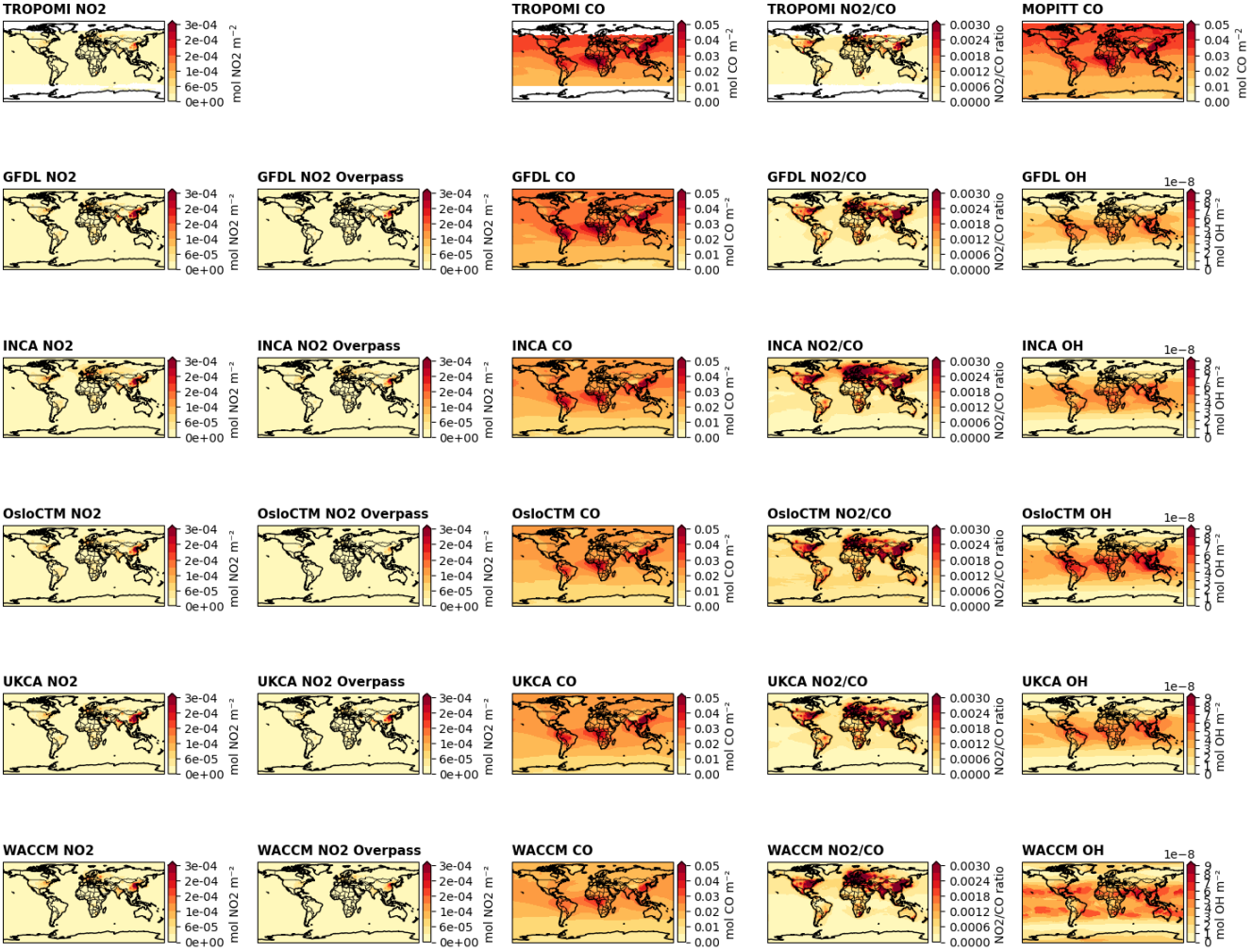

Figure A3: Similar to Fig. 3, but including a column estimating model NO_2 during overpass using the ratio of overpass time NO_2 to monthly mean NO_2 from the 3-hourly OsloCTM3 simulations. Global maps of annual mean satellite retrievals for (a) NO_2 for TROPOMI and models; (b) NO_2 for the models with monthly mean values multipled by the ratio of monthly mean:3-hourly values during overpass for OsloCTM3; (c) CO for MOPITT, TROPOMI and models; (d) NO_2/CO values in the models, and (e) OH in the models other than UCI.

https://doi.org/10.5194/egusphere-2025-4898
Preprint. Discussion started: 29 October 2025

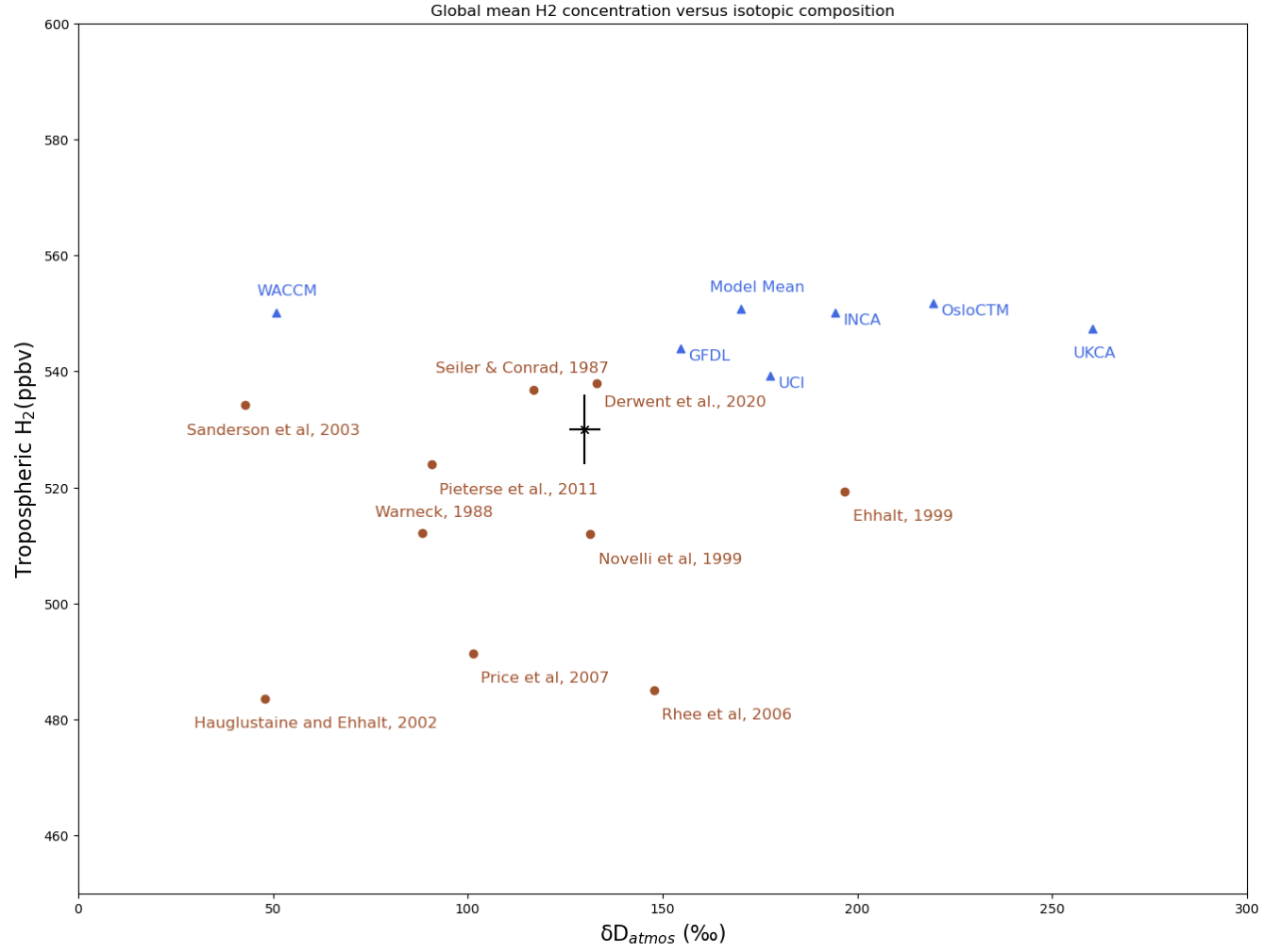

Figure A4: Similar to Fig. 8, but using isotopic fractionation factors for dry deposition and photochemical losses from (Pieterse et al., 2011)

https://doi.org/10.5194/egusphere-2025-4898
Preprint. Discussion started: 29 October 2025

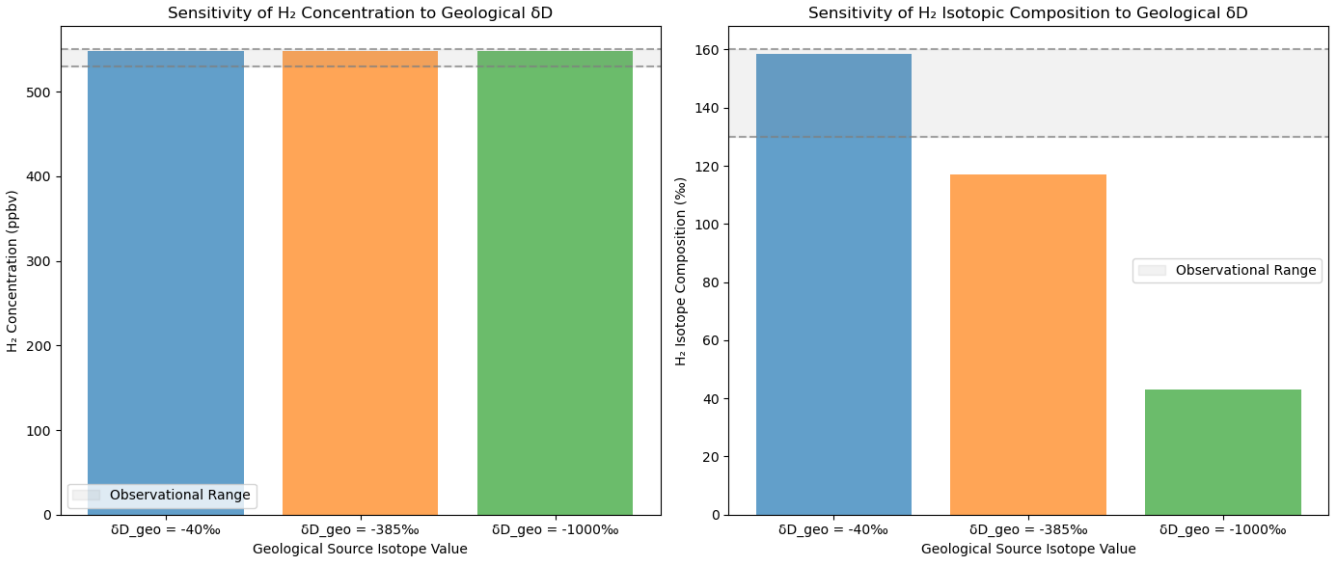

Figure A5: Effect of different isotopic compositions for a geological source of 9 Tg/yr.

Table A1: Parameter and input data for the box model. Values in this table is for the setup where the box model is adjusted to OsloCTM3 results from Sand et al. (2024). The model can be adjusted to other ACMs replacing OsloCTM3 values with values from Table 2.

Parameters	**Description and Reference**
Reference year (refyr = 2010)	Reference year for which the box model is calibrated to the OsloCTM3.
Pre-industrial concentration (pre_ind_conc = 330 ppb)	Pre-industrial (year 1850) concentration. Taken from Patterson et al. 2021.
Atmospheric production (prod_ref = 46.9 Tg/yr)	Total atmospheric H_2 production in reference year from OsloCTM3.
Soil sink lifetime (tau_2 = 3.3 years)	H_2 soil sink lifetime taken from the OsloCTM3 simulation representing the reference year.
Atmospheric lifetime (tau_1 = 6.9 years)	H_2 atmospheric lifetime taken from the OsloCTM3 simulation representing the reference year.
Nitrogen fixation (nit_fix = 9 Tg/yr)	Nitrogen fixation emissions from soil and ocean. Fixed for all years.
Natural VOC emissions (natvoc = 640,6Tg yr-1)	Natural VOC emissions. Fixed for all years.

https://doi.org/10.5194/egusphere-2025-4898
Preprint. Discussion started: 29 October 2025

Conversion from burden to concentration (beta_h2 = 0.37 ppb/Tg)	Convert mass of H_2 to concentration in ppb ($5.1352e^{9}$ * 2.0 / 28.97 * $1e^{-9}$)
Fraction of atmospheric production from VOC (frac_voc_org = 0.39)	Fraction of atmospheric H_2 production originating from VOC. (1-frac_voc_org) is due to CH_4. (Ehhalt and Rohrer, 2009; Paulot et al., 2024)
Anthropogenic H_2 emissions	Historical anthropogenic H_2 emissions (CEDS21; (Szopa et al., 2021))
Biomass burning H_2 emissions	Historical H_2 emissions from biomass burning taken from GFED4s (van der Werf et al., 2017). Prior to 1997 a value of 9.1 Tg/yr is used.
Methane concentration	Historical methane concentration. Used to scale the methane fraction of the atmospheric production of H_2 in time. (Meinshausen et al., 2017)
Anthropogenic VOC emissions	Historical non methane VOC emissions. Used to scale the VOC fraction of the atmospheric production of H_2 in time. (Hoesly et al., 2018)

Code availability

The box model is available at https://github.com/ciceroOslo/simpleH2/tree/simpleH2_plot_preprint_withiso

Author Contribution

S.K. led the study and the writing of the article. R.B.S., M.S. and S.K. designed and ran the box model. Ø.H. ran the WACCM model, S.K. ran the UCI CTM model, H.B. ran the UKCA model, D.H. ran the INCA model, and F.P. ran the GFDL model. All the above-mentioned and M.S., G.M., M.P., and D.S. contributed to the design of the study and discussions of the results. All authors contributed to the writing of the article.

https://doi.org/10.5194/egusphere-2025-4898
Preprint. Discussion started: 29 October 2025

Competing interests

G.M. is a member of the editorial board of Atmospheric Chemistry and Physics

Acknowledgments

The work has received funding from the Norwegian Research Council (80%) and and six industrial partners (20%): Shell, Equinor, Statkraft, Linde, Gassco and Norwegian Shipowners' Associations (HYDROGEN, grants no. 320240) and the European Union's Horizon Europe research and innovation programme under grant agreement no. 101137582 (HYway). The OsloCTM3 simulations were performed on resources provided by Sigma2 - the National Infrastructure for High Performance Computing and Data Storage in Norway (project account NN9188K).

References

Andreae, M. O. and Merlet, P.: Emission of trace gases and aerosols from biomass burning, Global Biogeochemical Cycles, 15, 955–966, https://doi.org/10.1029/2000GB001382, 2001.

Batenburg, A. M., Walter, S., Pieterse, G., Levin, I., Schmidt, M., Jordan, A., Hammer, S., Yver, C., and Röckmann, T.: Temporal and spatial variability of the stable isotopic composition of atmospheric molecular hydrogen: observations at six EUROHYDROS stations, Atmospheric Chemistry and Physics, 11, 6985–6999, https://doi.org/10.5194/acp-11-6985-2011, 2011.

Buzzard, V., Thorne, D., Gil-Loaiza, J., Cueva, A., and Meredith, L. K.: Sensitivity of soil hydrogen uptake to natural and managed moisture dynamics in a semiarid urban ecosystem, PeerJ, 10, e12966, https://doi.org/10.7717/peerj.12966, 2022.

Chance, K., Palmer, P. I., Spurr, R. J. D., Martin, R. V., Kurosu, T. P., and Jacob, D. J.: Satellite observations of formaldehyde over North America from GOME, Geophysical Research Letters, 27, 3461–3464, https://doi.org/10.1029/2000GL011857, 2000.

Conrad, R.: Soil microorganisms as controllers of atmospheric trace gases (H2, CO, CH4, OCS, N2O, and NO), Microbiological Reviews, 60, 609, https://doi.org/10.1128/mr.60.4.609-640.1996, 1996.

Conrad, R. and Babbel, M.: Effect of dilution on methanogenesis, hydrogen turnover and interspecies hydrogen transfer in anoxic paddy soil, FEMS Microbiology Letters, 62, 21–27, https://doi.org/10.1111/j.1574-6968.1989.tb03654.x, 1989.

Conrad, R. and Seiler, W.: Contribution of hydrogen production by biological nitrogen fixation to the global hydrogen budget, Journal of Geophysical Research: Oceans, 85, 5493–5498, https://doi.org/10.1029/JC085iC10p05493, 1980.

Dalsøren, S. B., Myhre, C. L., Myhre, G., Gomez-Pelaez, A. J., Søvde, O. A., Isaksen, I. S. A., Weiss, R. F., and Harth, C. M.: Atmospheric methane evolution the last 40 years, Atmospheric Chemistry and Physics, 16, 3099–3126, https://doi.org/10.5194/acp-16-3099-2016, 2016.

https://doi.org/10.5194/egusphere-2025-4898
Preprint. Discussion started: 29 October 2025

De Smedt, I., Müller, J.-F., Stavrakou, T., van der A, R., Eskes, H., and Van Roozendael, M.: Twelve years of global observations of formaldehyde in the troposphere using GOME and SCIAMACHY sensors, Atmospheric Chemistry and Physics, 8, 4947–4963, https://doi.org/10.5194/acp-8-4947-2008, 2008.

Deeter, M. N., Emmons, L. K., Francis, G. L., Edwards, D. P., Gille, J. C., Warner, J. X., Khattatov, B., Ziskin, D., Lamarque, J.-F., Ho, S.-P., Yudin, V., Attié, J.-L., Packman, D., Chen, J., Mao, D., and Drummond, J. R.: Operational carbon monoxide retrieval algorithm and selected results for the MOPITT instrument, Journal of Geophysical Research: Atmospheres, 108, https://doi.org/10.1029/2002JD003186, 2003.

Derwent, R. G. and Jenkin, M. E.: Estimation of the atmospheric hydrogen source from the oxidation of man-made and natural non-methane organic compounds using a Master Chemical Mechanism, Atmospheric Environment, 339, 120871, https://doi.org/10.1016/j.atmosenv.2024.120871, 2024.

Duncan, B. N., Logan, J. A., Bey, I., Megretskaia, I. A., Yantosca, R. M., Novelli, P. C., Jones, N. B., and Rinsland, C. P.: Global budget of CO, 1988–1997: Source estimates and validation with a global model, Journal of Geophysical Research: Atmospheres, 112, https://doi.org/10.1029/2007JD008459, 2007.

Ehhalt, D., Prather, M., Dentener, F., Derwent, R., Dlugokencky, E., Holland, E., Isaksen, I., Katima, J., Kirchhoff, V., Matson, P., Midgley, P., Wang, M., Berntsen, T., Bey, I., Brasseur, G., Buja, L., Collins, W. J., Daniel, J., DeMore, W. B., Derek, N., Dickerson, R., Etheridge, D., Feichter, J., Fraser, P., Friedl, R., Fuglestvedt, J., Gauss, M., Grenfell, L., Grübler, A., Harris, N., Hauglustaine, D., Horowitz, L., Jackman, C., Jacob, D., Jaeglé, L., Jain, A., Kanakidou, M., Karlsdottir, S., Ko, M., Kurylo, M., Lawrence, M., Logan, J. A., Manning, M., Mauzerall, D., McConnell, J., Mickley, L., Montzka, S., Müller, J. F., Olivier, J., Pickering, K., Pitari, G., Roelofs, G. J., Rogers, H., Rognerud, B., Smith, S., Solomon, S., Staehelin, J., Steele, P., Stevenson, D., Sundet, J., Thompson, A., van Weele, M., Joos, F., and McFarland, M.: Atmospheric Chemistry and Greenhouse Gases, in: Climate Change 2001: The Scientific Basis. Contribution of Working Group I to the Third Assessment Report of the Intergovernmental Panel on Climate Change, Cambridge University Press, 239–288, 2001.

Ehhalt, D. H. and Rohrer, F.: The tropospheric cycle of H2: a critical review, Tellus B: Chemical and Physical Meteorology, 61, 500–535, https://doi.org/10.1111/j.1600-0889.2009.00416.x, 2009.

Esquivel-Elizondo, S., Hormaza Mejia, A., Sun, T., Shrestha, E., Hamburg, S. P., and Ocko, I. B.: Wide range in estimates of hydrogen emissions from infrastructure, Front. Energy Res., 11, https://doi.org/10.3389/fenrg.2023.1207208, 2023.

Gerst, S. and Quay, P.: Deuterium component of the global molecular hydrogen cycle, Journal of Geophysical Research: Atmospheres, 106, 5021–5031, https://doi.org/10.1029/2000JD900593, 2001.

Gibson, J. J., Eby, P., and Jaggi, A.: Natural isotope fingerprinting of produced hydrogen and its potential applications to the hydrogen economy, International Journal of Hydrogen Energy, 66, 468–478, https://doi.org/10.1016/j.ijhydene.2024.04.077, 2024.

Hagemann, R., Nief, G., and Roth, E.: Absolute isotopic scale for deuterium analysis of natural waters. Absolute D/H ratio for SMOW, Tellus, 22, 712–715, https://doi.org/10.1111/j.2153-3490.1970.tb00540.x, 1970.

Hauglustaine, D. A. and Ehhalt, D. H.: A three-dimensional model of molecular hydrogen in the troposphere, Journal of Geophysical Research: Atmospheres, 107, ACH 4-1-ACH 4-16, https://doi.org/10.1029/2001JD001156, 2002.

Hoesly, R. M., Smith, S. J., Feng, L., Klimont, Z., Janssens-Maenhout, G., Pitkanen, T., Seibert, J. J., Vu, L., Andres, R. J., Bolt, R. M., Bond, T. C., Dawidowski, L., Kholod, N., Kurokawa, J., Li, M., Liu, L., Lu, Z., Moura, M. C. P., O'Rourke, P. R., and Zhang, Q.: Historical (1750–2014) anthropogenic emissions of reactive gases and aerosols from the Community

https://doi.org/10.5194/egusphere-2025-4898
Preprint. Discussion started: 29 October 2025

Emissions Data System (CEDS), Geoscientific Model Development, 11, 369–408, https://doi.org/10.5194/gmd-11-369-2018, 2018.

Lama, S., Houweling, S., Boersma, K. F., Aben, I., Denier van der Gon, H. A. C., and Krol, M. C.: Estimation of OH in urban plumes using TROPOMI-inferred NO_2 / CO, Atmospheric Chemistry and Physics, 22, 16053–16071, https://doi.org/10.5194/acp-22-16053-2022, 2022.

Meinshausen, M., Vogel, E., Nauels, A., Lorbacher, K., Meinshausen, N., Etheridge, D. M., Fraser, P. J., Montzka, S. A., Rayner, P. J., Trudinger, C. M., Krummel, P. B., Beyerle, U., Canadell, J. G., Daniel, J. S., Enting, I. G., Law, R. M., Lunder, C. R., O'Doherty, S., Prinn, R. G., Reimann, S., Rubino, M., Velders, G. J. M., Vollmer, M. K., Wang, R. H. J., and Weiss, R.: Historical greenhouse gas concentrations for climate modelling (CMIP6), Geoscientific Model Development, 10, 2057–2116, https://doi.org/10.5194/gmd-10-2057-2017, 2017.

Novelli, P. C., Lang, P. M., Masarie, K. A., Hurst, D. F., Myers, R., and Elkins, J. W.: Molecular hydrogen in the troposphere: Global distribution and budget, Journal of Geophysical Research: Atmospheres, 104, 30427–30444, https://doi.org/10.1029/1999JD900788, 1999.

Patterson, J. D., Aydin, M., Crotwell, A. M., Petron, G., Severinghaus, J. P., and Saltzman, E. S.: Atmospheric History of H2 Over the Past Century Reconstructed From South Pole Firn Air, Geophysical Research Letters, 47, e2020GL087787, https://doi.org/10.1029/2020GL087787, 2020.

Patterson, J. D., Aydin, M., Crotwell, A. M., Pétron, G., Severinghaus, J. P., Krummel, P. B., Langenfelds, R. L., and Saltzman, E. S.: H2 in Antarctic firn air: Atmospheric reconstructions and implications for anthropogenic emissions, Proceedings of the National Academy of Sciences, 118, e2103335118, https://doi.org/10.1073/pnas.2103335118, 2021.

Paulot, F., Paynter, D., Naik, V., Malyshev, S., Menzel, R., and Horowitz, L. W.: Global modeling of hydrogen using GFDL-AM4.1: Sensitivity of soil removal and radiative forcing, International Journal of Hydrogen Energy, 46, 13446–13460, https://doi.org/10.1016/j.ijhydene.2021.01.088, 2021.

Paulot, F., Pétron, G., Crotwell, A. M., and Bertagni, M. B.: Reanalysis of NOAA H_2 observations: implications for the H_2 budget, Atmospheric Chemistry and Physics, 24, 4217–4229, https://doi.org/10.5194/acp-24-4217-2024, 2024.

Pérez-Peña, M. P., Fisher, J. A., Millet, D. B., Yashiro, H., Langenfelds, R. L., Krummel, P. B., and Kable, S. H.: Evaluating the contribution of the unexplored photochemistry of aldehydes on the tropospheric levels of molecular hydrogen (H_2), Atmospheric Chemistry and Physics, 22, 12367–12386, https://doi.org/10.5194/acp-22-12367-2022, 2022.

Pétron, G., Crotwell, A. M., Mund, J., Crotwell, M., Mefford, T., Thoning, K., Hall, B., Kitzis, D., Madronich, M., Moglia, E., Neff, D., Wolter, S., Jordan, A., Krummel, P., Langenfelds, R., and Patterson, J.: Atmospheric H_2 observations from the NOAA Cooperative Global Air Sampling Network, Atmospheric Measurement Techniques, 17, 4803–4823, https://doi.org/10.5194/amt-17-4803-2024, 2024.

Pieterse, G., Krol, M. C., and Röckmann, T.: A consistent molecular hydrogen isotope chemistry scheme based on an independent bond approximation, Atmospheric Chemistry and Physics, 9, 8503–8529, https://doi.org/10.5194/acp-9-8503-2009, 2009.

Pieterse, G., Krol, M. C., Batenburg, A. M., Steele, L. P., Krummel, P. B., Langenfelds, R. L., and Röckmann, T.: Global modelling of H_2 mixing ratios and isotopic compositions with the TM5 model, Atmospheric Chemistry and Physics, 11, 7001–7026, https://doi.org/10.5194/acp-11-7001-2011, 2011.

https://doi.org/10.5194/egusphere-2025-4898
Preprint. Discussion started: 29 October 2025

Pieterse, G., Krol, M. C., Batenburg, A. M., M. Brenninkmeijer, C. A., Popa, M. E., O'Doherty, S., Grant, A., Steele, L. P., Krummel, P. B., Langenfelds, R. L., Wang, H. J., Vermeulen, A. T., Schmidt, M., Yver, C., Jordan, A., Engel, A., Fisher, R. E., Lowry, D., Nisbet, E. G., Reimann, S., Vollmer, M. K., Steinbacher, M., Hammer, S., Forster, G., Sturges, W. T., and Röckmann, T.: Reassessing the variability in atmospheric H2 using the two-way nested TM5 model, Journal of Geophysical Research: Atmospheres, 118, 3764–3780, https://doi.org/10.1002/jgrd.50204, 2013.

Price, H., Jaeglé, L., Rice, A., Quay, P., Novelli, P. C., and Gammon, R.: Global budget of molecular hydrogen and its deuterium content: Constraints from ground station, cruise, and aircraft observations, Journal of Geophysical Research: Atmospheres, 112, https://doi.org/10.1029/2006JD008152, 2007.

Prinn, R. G., Weiss, R. F., Miller, B. R., Huang, J., Alyea, F. N., Cunnold, D. M., Fraser, P. J., Hartley, D. E., and Simmonds, P. G.: Atmospheric Trends and Lifetime of CH3CCI3 and Global OH Concentrations, Science, 269, 187–192, https://doi.org/10.1126/science.269.5221.187, 1995.

Rhee, T. S., Brenninkmeijer, C. a. M., and Röckmann, T.: The overwhelming role of soils in the global atmospheric hydrogen cycle, Atmospheric Chemistry and Physics, 6, 1611–1625, https://doi.org/10.5194/acp-6-1611-2006, 2006.

Rhee, T. S., Brenninkmeijer, C. a. M., and Röckmann, T.: Hydrogen isotope fractionation in the photolysis of formaldehyde, Atmospheric Chemistry and Physics, 8, 1353–1366, https://doi.org/10.5194/acp-8-1353-2008, 2008.

Rice, A. L. and Quay, P.: Isotopic Composition of Formaldehyde in Urban Air, Environ. Sci. Technol., 43, 8752–8758, https://doi.org/10.1021/es9010916, 2009.

Röckmann, T., Gómez Álvarez, C. X., Walter, S., van der Veen, C., Wollny, A. G., Gunthe, S. S., Helas, G., Pöschl, U., Keppler, F., Greule, M., and Brand, W. A.: Isotopic composition of H2 from wood burning: Dependency on combustion efficiency, moisture content, and δD of local precipitation, Journal of Geophysical Research: Atmospheres, 115, https://doi.org/10.1029/2009JD013188, 2010.

Sand, M., Skeie, R. B., Sandstad, M., Krishnan, S., Myhre, G., Bryant, H., Derwent, R., Hauglustaine, D., Paulot, F., Prather, M., and Stevenson, D.: A multi-model assessment of the Global Warming Potential of hydrogen, Commun Earth Environ, 4, 203, https://doi.org/10.1038/s43247-023-00857-8, 2023.

Sanderson, M. G., Collins, W. J., Derwent, R. G., and Johnson, C. E.: Simulation of Global Hydrogen Levels Using a Lagrangian Three-Dimensional Model, Journal of Atmospheric Chemistry, 46, 15–28, https://doi.org/10.1023/A:1024824223232, 2003.

Skeie, R. B., Hodnebrog, Ø., and Myhre, G.: Trends in atmospheric methane concentrations since 1990 were driven and modified by anthropogenic emissions, Commun Earth Environ, 4, 1–14, https://doi.org/10.1038/s43247-023-00969-1, 2023.

Stevenson, D. S., Zhao, A., Naik, V., O'Connor, F. M., Tilmes, S., Zeng, G., Murray, L. T., Collins, W. J., Griffiths, P. T., Shim, S., Horowitz, L. W., Sentman, L. T., and Emmons, L.: Trends in global tropospheric hydroxyl radical and methane lifetime since 1850 from AerChemMIP, Atmospheric Chemistry and Physics, 20, 12905–12920, https://doi.org/10.5194/acp-20-12905-2020, 2020.

Szopa, S., Naik, V., Adhikary, B., Artaxo, P., Berntsen, T., Collins, W. D., Fuzzi, S., Gallardo, L., Kiendler-Scharr, A., Klimont, Z., Liao, H., Unger, N., and Zanis, P.: Short-Lived Climate Forcers (Chapter 6), in: IPCC 2021: Climate Change 2021: The Physical Science Basis. Contribution of Working Group I to the Sixth Assessment Report of the Intergovernmental Panel on Climate Change, edited by: Masson-Delmotte, V., Zhai, P., Pirani, A., Connors, S. L., Péan, C., Berger, S., Caud, N., Chen, Y., Goldfarb, L., Gomis, M. I., Huang, M., Leitzell, K., Lonnoy, E., Matthews, J. B. R.,

https://doi.org/10.5194/egusphere-2025-4898
Preprint. Discussion started: 29 October 2025

595 Maycock, T. K., Waterfield, T., Yelek\cci, K., Yu, R., and Zhu, B., Cambridge University Press, Cambridge, United Kingdom and New York, NY, USA, 817–922, https://doi.org/10.1017/9781009157896.008, 2021.

Trapani, D., Marocco, P., Gandiglio, M., and Santarelli, M.: Hydrogen leakages across the supply chain: Current estimates and future scenarios, International Journal of Hydrogen Energy, 145, 1084–1095, https://doi.org/10.1016/j.ijhydene.2025.06.103, 2025.

600 Veefkind, J. P., Aben, I., McMullan, K., Förster, H., de Vries, J., Otter, G., Claas, J., Eskes, H. J., de Haan, J. F., Kleipool, Q., van Weele, M., Hasekamp, O., Hoogeveen, R., Landgraf, J., Snel, R., Tol, P., Ingmann, P., Voors, R., Kruizinga, B., Vink, R., Visser, H., and Levelt, P. F.: TROPOMI on the ESA Sentinel-5 Precursor: A GMES mission for global observations of the atmospheric composition for climate, air quality and ozone layer applications, Remote Sensing of Environment, 120, 70–83, https://doi.org/10.1016/j.rse.2011.09.027, 2012.

605 Vollmer, M. K., Walter, S., Bond, S. W., Soltic, P., and Röckmann, T.: Molecular hydrogen (H_2) emissions and their isotopic signatures (H/D) from a motor vehicle: implications on atmospheric H_2, Atmospheric Chemistry and Physics, 10, 5707–5718, https://doi.org/10.5194/acp-10-5707-2010, 2010.

Walter, S., Laukenmann, S., Stams, A. J. M., Vollmer, M. K., Gleixner, G., and Röckmann, T.: The stable isotopic signature of biologically produced molecular hydrogen (H_2), Biogeosciences, 9, 4115–4123, https://doi.org/10.5194/bg-9-4115-2012,
610 2012.

van der Werf, G. R., Randerson, J. T., Giglio, L., van Leeuwen, T. T., Chen, Y., Rogers, B. M., Mu, M., van Marle, M. J. E., Morton, D. C., Collatz, G. J., Yokelson, R. J., and Kasibhatla, P. S.: Global fire emissions estimates during 1997–2016, Earth System Science Data, 9, 697–720, https://doi.org/10.5194/essd-9-697-2017, 2017.

Xiao, X., Prinn, R. G., Simmonds, P. G., Steele, L. P., Novelli, P. C., Huang, J., Langenfelds, R. L., O'Doherty, S.,
615 Krummel, P. B., Fraser, P. J., Porter, L. W., Weiss, R. F., Salameh, P., and Wang, R. H. J.: Optimal estimation of the soil uptake rate of molecular hydrogen from the Advanced Global Atmospheric Gases Experiment and other measurements, Journal of Geophysical Research: Atmospheres, 112, https://doi.org/10.1029/2006JD007241, 2007.

Yang, L. H., Jacob, D. J., Lin, H., Dang, R., Bates, K. H., East, J. D., Travis, K. R., Pendergrass, D. C., and Murray, L. T.: Assessment of Hydrogen's Climate Impact Is Affected by Model OH Biases, Geophysical Research Letters, 52,
620 e2024GL112445, https://doi.org/10.1029/2024GL112445, 2025.

Yver, C. E., Pison, I. C., Fortems-Cheiney, A., Schmidt, M., Chevallier, F., Ramonet, M., Jordan, A., Søvde, O. A., Engel, A., Fisher, R. E., Lowry, D., Nisbet, E. G., Levin, I., Hammer, S., Necki, J., Bartyzel, J., Reimann, S., Vollmer, M. K., Steinbacher, M., Aalto, T., Maione, M., Arduini, J., O'Doherty, S., Grant, A., Sturges, W. T., Forster, G. L., Lunder, C. R., Privalov, V., Paramonova, N., Werner, A., and Bousquet, P.: A new estimation of the recent tropospheric molecular
625 hydrogen budget using atmospheric observations and variational inversion, Atmospheric Chemistry and Physics, 11, 3375–3392, https://doi.org/10.5194/acp-11-3375-2011, 2011.

Zgonnik, V.: The occurrence and geoscience of natural hydrogen: A comprehensive review, Earth-Science Reviews, 203, 103140, https://doi.org/10.1016/j.earscirev.2020.103140, 2020.

Zimmerman, P. R., Greenberg, J. P., Wandiga, S. O., and Crutzen, P. J.: Termites: A Potentially Large Source of
630 Atmospheric Methane, Carbon Dioxide, and Molecular Hydrogen, Science, 218, 563–565, https://doi.org/10.1126/science.218.4572.563, 1982.